



## Research papers

# Glacier mass balance and its potential impacts in the Altai Mountains over the period 1990–2011



Yong Zhang<sup>a,b,c,\*</sup>, Hiroyuki Enomoto<sup>b</sup>, Tetsuo Ohata<sup>b</sup>, Hideyuki Kitabata<sup>d</sup>, Tsutomu Kadota<sup>d</sup>, Yukiko Hirabayashi<sup>e</sup>

<sup>a</sup>School of Resource Environment and Safety Engineering, Hunan University of Science and Technology, Xiangtan 411201, China

<sup>b</sup>Arctic Environment Research Center, National Institute of Polar Research, Tokyo 190-8518, Japan

<sup>c</sup>State Key Laboratory of Cryospheric Science, Northwest Institute of Eco-Environment and Resources, Chinese Academy of Sciences, Lanzhou 730000, China

<sup>d</sup>Japan Agency for Marine–Earth Science and Technology, Yokohama 237-0061, Japan

<sup>e</sup>Institute of Industrial Science, The University of Tokyo, Tokyo 153-8505, Japan

## ARTICLE INFO

## Article history:

Received 20 January 2017

Received in revised form 30 July 2017

Accepted 17 August 2017

Available online 26 August 2017

This manuscript was handled by K.

Georgakakos, Editor-in-Chief, with the assistance of Daqing Yang, Associate Editor.

## Keywords:

Mass balance

WRF data

Water resources

Altai Mountains

## ABSTRACT

The Altai Mountains contain 1281 glaciers covering an area of 1191 km<sup>2</sup>. These glaciers have undergone significant changes in glacial length and area over the past decade. However, mass changes of these glaciers and their impacts remain poorly understood. Here we present surface mass balances of all glaciers in the region for the period 1990–2011, using a glacier mass-balance model forced by the outputs of a regional climate model. Our results indicate that the mean specific mass balance for the whole region is about  $-0.69$  m w.e. yr<sup>-1</sup> over the entire period, and about 81.3% of these glaciers experience negative net mass balance. We detect an accelerated wastage of these glaciers in recent years, and marked differences in mass change and its sensitivity to climate change for different regions and size classes. In particular, higher mass loss and temperature sensitivity are observed for glaciers smaller than 0.5 km<sup>2</sup>. In addition to temperature rise, a decrease in precipitation in the western part of the region and an increase in precipitation in the eastern part likely contribute to significant sub-region differences in mass loss. With significant glacier wastage, the contribution of all glaciers to regional water resources and sea-level change becomes larger than before, but may not be a potential threat to human populations through impacts on water availability.

© 2017 Elsevier B.V. All rights reserved.

## 1. Introduction

The Altai Mountains, a region with large ice bodies, are mountains comprising the westernmost extent of Mongolia, and the common border regions of north-western China, eastern Kazakhstan, and Russia. The region rises from 2000 m above sea level (a.s.l.) in the north-western Altai to more than 4500 m a.s.l. in the central plateau of the Russian Altai Mountains, in which glaciers are primarily distributed in the Katun and Chuya Ridges, the Tavan Bogd Range, and the Kharkhiraa and Tsambagarav massifs (Fig. 1). These glaciers are an important source of freshwater for the upper tributaries of the Ob, Irtysh and Yenisei rivers (Wang and Cho, 1997; Li et al., 2010; Pan, 2013). Their role in local water supply becomes especially important in semi-arid and arid regions that seasonally lack sufficient water supply from precipita-

tion (Kaser et al., 2010; Viviroli et al., 2011). Glaciers in the Mongolian Altai Mountains provide an estimated 10.8% of the total water resources within the Mongolia (Pan, 2013), and these in the Chinese Altai Mountains contribute 7.7% of the total runoff of the Irtysh River (Li et al., 2010). In addition, the contribution to sea-level change from these glaciers has grown during the past decades (Dyurgerov, 2010; Radić and Hock, 2011).

Recent investigations of glacier fluctuations in the Altai Mountains indicate a significant, continued shrinkage of the glaciers over the past decades (Kadota and Gombo, 2007; Surazakov et al., 2007; Shahgedanova et al., 2010; Kadota et al., 2011; Narozhniy and Zemtsov, 2011; Yao et al., 2012; Konya et al., 2013; Krumwiede et al., 2014; Syromyatina et al., 2015; Wei et al., 2015). Glacier area decreased by 9.0–27.0% in the Russian Altai Mountains for the period 1952–2008 (Narozhniy and Zemtsov, 2011), by 10.0–30.0% in the Mongolian Altai Mountains since the 1950s (Kadota and Gombo, 2007), and by 36.9% in the Chinese Altai Mountains for the period 1960–2009 (Yao et al., 2012). In particular, decline in glacier area is more pronounced in the Chinese Altai Mountains

\* Corresponding author at: School of Resource Environment and Safety Engineering, Hunan University of Science and Technology, Xiangtan 411201, China.

E-mail address: [yong.zhang@hnust.edu.cn](mailto:yong.zhang@hnust.edu.cn) (Y. Zhang).

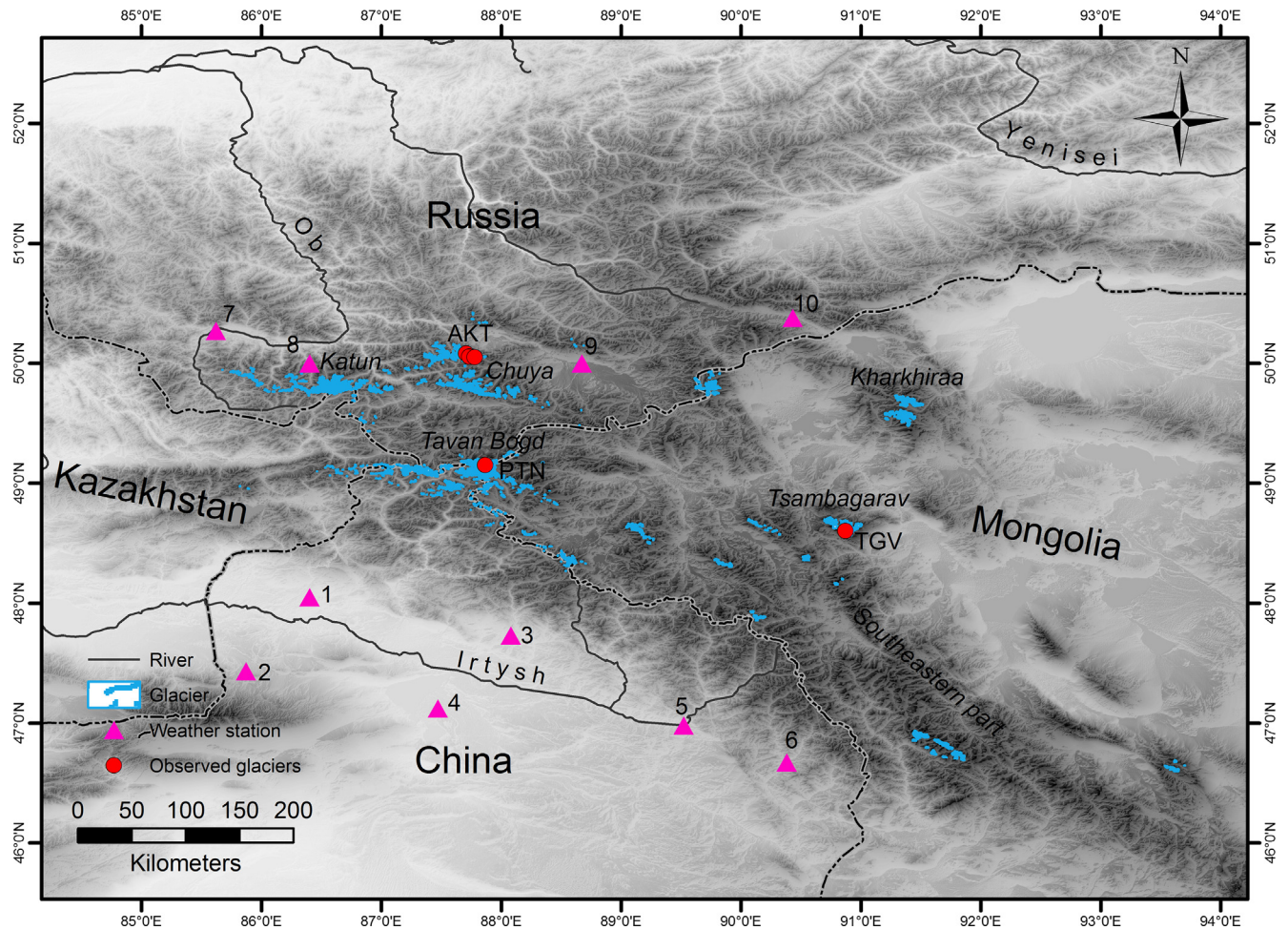


**Fig. 1.** Location of the Altai Mountains and glacier distribution. Abbreviations refer to: AKT, Aktru River Basin (including Leviiy Aktru (LA), Maliy Aktru (MA), and Praviy Aktru (PA) and Vodopadnyi (VP) glaciers); PTN, Potanin Glacier; TGV, Tsambagarav Glacier. No. 1–10 show the weather stations, which are Habahe, Jimunai, Aletai, Fuhai, Fuwen, Qinghe, Ust-Coksa, Kara-Tureck, Kosh-Agach and Mugur-Aksy, respectively.

than those in other mountain systems of the Tibetan Plateau and surroundings (Yao et al., 2012; Wei et al., 2015). Consequently, glacier wastage in this region has had many impacts on matters ranging from regional sustainability of water supplies and ecosystem to global sea-level change.

So far, studies on the Altai glaciers have focused mainly on changes in glacier area and length (e.g., Kadota and Gombo, 2007; Surazakov et al., 2007; Shahgedanova et al., 2010; Kadota et al., 2011; Yao et al., 2012; Krumwiede et al., 2014; Syromyatina et al., 2015; Wei et al., 2015), but an up-to-date regional assessment of surface mass balances for these glaciers is missing. The surface mass balance of a glacier is particularly important in the context of the links between glacier and climate change (Oerlemans and Fortuin, 1992; Braithwaite et al., 2002; Cuffey and Paterson, 2010). In fact, the surface mass balance is more closely related to the atmospheric forcing compared to changes in glacier area and length, thus providing an opportunity to understand glacier-climate interactions. However, in situ observations of surface mass balances have been carried out only on six glaciers in the entire Altai Mountains during different periods (Table 1), and these glaciers cover less than ~4% of the total glacier area. Of these records, two start in 2005 and 2008, and four are located in a river basin (Table 1). These field observations in the same basin only allow for the detection of one climate change signal for this region, however, climatic regimes of the region vary from the wet conditions of the northwest to the dry conditions of the southeast

(Klinge et al., 2003). Therefore, the lack of temporally and spatially long-term information about variations in glacier mass balance in the Altai Mountains hampers the possibility of gaining insights into the mechanisms driving these changes; on the other hand, these field observations of surface mass balances in the region treated as regionally representative for global estimation of glacier mass balance may lead to substantial uncertainties due to the short time spans and unevenly distribution of these field records. For a better understanding of how glaciers have been changing when subjected to climate change on a multi-decadal scale, quantitative assessment of glacier mass balance for the whole Altai Mountains is a pressing need.

Furthermore, the availability of hydrometeorological data sets in high-elevation regions of the Altai Mountains is extremely limited. In particular, there is little information about the variability in space and time of temperature and precipitation in these high-elevation regions. To overcome this problem, one way is through the use of regional climate model (RCM) outputs. In a number of studies, RCM outputs have been used as forcing data for large-scale modelling of glacier mass balance (e.g., Machguth et al., 2009; Mölg and Kaser, 2011; Mölg et al., 2012, 2013; Collier et al., 2013; Ligtenberg et al., 2013; Lang et al., 2015; Möller et al., 2016). Among the available RCMs, the Weather Research and Forecast (WRF) model is often used to address the issue of spatial resolution to generate climate data in different regions (Mausson et al., 2011; Mölg et al., 2012, 2013; Collier et al.,

**Table 1**  
Characteristics of monitored glaciers in the Altai Mountains. Glacier information is from the GAMDAM Glacier Inventory (Nuimura et al., 2015) and the RGI (Arendt et al., 2014).

Glacier	Region	Elevation (m a.s.l.)	Length (km)	Area (km <sup>2</sup> )	Observed period
Leviy Aktru (LA)	Aktru basin	2665–4030	5.9	5.95	1977–2011
Maliy Aktru (MA)	Aktru basin	2267–3710	4.4	2.73	1962–2011
Praviy Aktru (PA) <sup>a</sup>	Aktru basin	2445–3668	5.3	3.88	1980–1990
Vodopadnyi (VP)	Aktru basin	2716–3549	1.4	0.98	1977–2011
Potanin	Tavan Bogd	2831–4241	10.4	24.81	2005/08–2012
Tsambagarav	Tsambagarav massif	3160–3800	3.6	7.2	2008–2011

<sup>a</sup> Observations on Praviy Aktru is not used due to different periods for measurement and simulation.

2013; Gao et al., 2015; Möller et al., 2016). This model provides high spatial-resolution forcing data for glacier mass balance simulation without statistical downscaling (Mölg et al., 2012, 2013; Collier et al., 2013). In particular, the increased resolution allows for improved representation of local features (Maussion et al., 2011).

In this study, we present variation in the surface mass balance of each of the Altai glaciers for the period 1990–2011 using a glacier mass-balance model. Outputs from the WRF model with 5 km resolution are used as an input for a 22-year run of the glacier mass-balance model for the entire Altai Mountains. The aim of this study is not only to compute mass balance distribution over entire mountain ranges but also to assess the role of these glaciers in regional water supply and the contribution to sea-level change. This, in turn, allows us to analyze differences in surface mass balance and its response to climate change for different sized glaciers and how patterns of their sensitivity to climate change at the mountain-range scale. Overall, our study provides an integrated view of the main patterns and forcings of glacier mass changes in the Altai Mountains, where some basic questions are still poorly known regarding the glacier-climate relationship.

## 2. Study area

The Altai Mountains have 1281 glaciers with a total area of 1191 km<sup>2</sup> (Arendt et al., 2014; Nuimura et al., 2015). Glaciers span an elevation range of 2000–4500 m a.s.l., within which nearly 80% of glacier area lies between 2800 and 3700 m a.s.l. (Fig. 2a). The size class of glaciers smaller than 0.5 km<sup>2</sup> dominates in terms of the total number, while covering only 13.8% of the total area (Fig. 2b). Most of the area is concentrated in the glaciers belonging to the size class of 1.0–5.0 km<sup>2</sup>, covering 44.1% of the total area (Fig. 2b). Small glaciers (<0.5 km<sup>2</sup>) are predominant in the Katun and Chuya Ridges and the Tavan Bogd Range, while they are sparser in the Mongolian Altai Mountains.

The region is under the influence of two wind systems: the westerly circulation in summer and the Siberian High in winter (Panagiotopoulos et al., 2005). Westerly flow dominates in summer (April–October), and humid air masses from the Atlantic Ocean and recycled moisture are the main sources of precipitation (Aizen et al., 2006). In winter (November–March), the region, located close to the center of the Siberian High, is dominated by high atmospheric pressure blocking the westerly flow (Panagiotopoulos et al., 2005), resulting in widespread extreme cold and dry conditions. The precipitation decreases from the western part to the eastern part of the region (Klinge et al., 2003; Narozhnyi and Zemtsov, 2011), and winter precipitation accounts for 10–30% of annual totals (Surazakov et al., 2007; Shahgedanova et al., 2010).

Meteorological observations indicate that increases in air temperature vary strongly between different regions, which are from 0.6 to 1.1 °C (Surazakov et al., 2007; Shahgedanova et al., 2010; Narozhnyi and Zemtsov, 2011; Bezuglova et al., 2012; Yao et al., 2012), while precipitation shows a complicated trend during recent decades (Surazakov et al., 2007; Shahgedanova et al.,

2010; Narozhnyi and Zemtsov, 2011; Wei et al., 2015; Malygina et al., 2017). Multiproxy reconstructions of past climate (e.g., Henderson et al., 2006; Kalugin et al., 2007; Okamoto et al., 2011) also indicate that the region has experienced significant warming since the Little Ice Age minimum.

## 3. Data

We use various data sets, including mass balance observations, geodetic mass changes, change rate in glacier area, and daily precipitation and temperature simulated by the WRF model and observed at ten weather stations. These data sets are briefly described below.

### 3.1. Mass balance

Direct observations of surface mass balance are available on six glaciers in the study region. Four of these glaciers, Leviy Aktru, Maliy Aktru, Praviy Aktru and Vodopadnyi (No. 125) glaciers, are located in the Aktru River Basin of the Northern Chuya Ridge (Table 1), the data of which are obtained from the World Glacier Monitoring Service (WGMS, 2014). The data of two glaciers, Potanin and Tsambagarav glaciers located in the Tavan Bogd Range and the Tsambagarav massif (Fig. 1), are derived from previous studies (Kadota et al., 2011; Konya et al., 2013). Due to different periods of measurement and simulation, the record of Praviy Aktru Glacier is not used in this study. In addition to Praviy Aktru Glacier, Leviy Aktru, Maliy Aktru, and Vodopadnyi glaciers have continuous and uninterrupted observations since the 1960s (Table 1). In the following analysis, the time series of glacier mass balance of the Aktru River Basin is averaged from the observations on above three glaciers over the period 1990–2011.

### 3.2. Geodetic mass change

Glacier-specific geodetic mass changes for the period 1999–2008 are available for the fourteen glaciers in the Chinese Altai Mountains from Wei et al. (2015). They intersected the Shuttle Radar Topography Mission (SRTM) Digital Elevation Model and the Advanced Space-borne Thermal Emission and Reflection Radiometer (ASTER) stereo images with glacier outlines to calculate geodetic mass balance. The average uncertainty in annual geodetic mass balance of these glaciers is estimated as  $\pm 0.13$  m water equivalent (w.e.) yr<sup>-1</sup> (Wei et al., 2015). The details of these data and glaciers can be found in the study of Wei et al. (2015).

### 3.3. Glacier area change

Reduction rates in area of the eighteen glaciers are available in two regions, which are derived from satellite data (Narozhnyi and Zemtsov, 2011; Wei et al., 2015). Fourteen of these glaciers are located in the Chinese Altai Mountains, the area change of which is estimated for the period 2000–2008 (Wei et al., 2015). The four glaciers are located in the Aktru River basin, the area change of

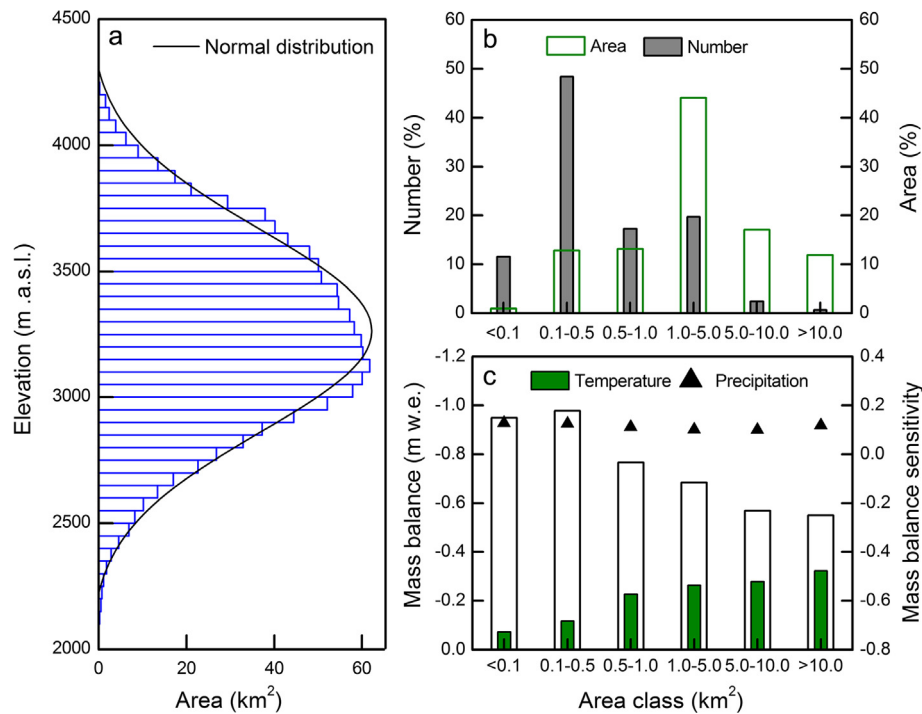


**Fig. 2.** (a) Area-altitude distribution of the Altai glaciers, (b) glacier distribution for different area size classes and (c) mass balance and sensitivities to temperature and precipitation changes for different area size classes.

which is calculated for the period 1999–2008 (Narozhniy and Zemtsov, 2011). We use these data to validate the model capability of capturing the feedback between glacier mass balance and change in glacier area. The details of these data and glaciers can be found in Narozhniy and Zemtsov (2011) and Wei et al. (2015), respectively.

**3.4. Meteorological data**

To reconstruct variation in the surface mass balance of the Altai glaciers, we use daily data sets of precipitation and near-surface temperature simulated by the Advanced Research version of the WRF version 3.4 (Skamarock et al., 2008). The WRF model is a fully compressible and nonhydrostatic model (Skamarock and Klemp, 2008; Skamarock et al., 2008), further information of which can be found in Skamarock et al. (2008). The WRF model was performed for a domain of 1000 km × 1000 km covering the whole Altai Mountains with 45 vertical levels (Kitabata et al., 2014). WRF outputs are available in the study region for the period 1988–2011 (Kitabata et al., 2014). Its spatial resolution is 5 km.

Surface air temperature and precipitation observations obtained from ten weather stations in the study region (Fig. 1

and Table 2) are used to evaluate the WRF outputs. Six weather stations are located in the Chinese Altai Mountains (Fig. 1), data of which are provided by the National Climate Center of China Meteorological Administration. Four weather stations are located in the Russian Altai Mountains (Fig. 1), data of which are provided by the official site of Administration and All-Russia Research Institute of Hydrometeorological Information-World Data Centre (RIHMI-WDC). The details of these stations are indicated in Table 2. Measurements of daily air temperature and precipitation are available for the period 1990–2011. Most weather stations have the slight elevation difference with the WRF grid points nearest to the weather stations (Table 2). In the following comparison, the time series of surface air temperature and precipitation over the study period averaged from the observations at ten weather stations is used.

**4. Methods**

**4.1. Glacial and meteorological data pre-processing**

Glacier area, length and elevation range (mean, maximum and minimum elevations) needed for the model are extracted from

**Table 2**

Summary of ten weather stations collected around the Altai Mountains. Lon, Lat, and Alt indicate the longitude (°E), latitude (°N) and altitude (m a.s.l.). The location of these stations is shown in Fig. 1.

No.	Name	Lon	Lat	Alt	WRF Alt
1	HABAHE	86.40	48.05	534.0	503.0
2	JIMUNAI	85.87	47.43	984.0	1150.0
3	ALETAI	88.08	47.73	736.9	749.0
4	FUHAI	87.47	47.12	502.0	496.0
5	FUWEN	89.52	46.98	826.6	828.0
6	QINHE	90.38	46.47	1220.0	1280.0
7	UST-COKSA	85.62	50.27	977.0	1647.0
8	KARA-TURECK	86.40	50.00	2600.0	1919.0
9	KOSH-AGACH	88.67	50.00	1759.0	1754.0
10	MUGUR-AKSY	95.12	50.27	1100.0	1798.0

the Glacier Area Mapping for Discharge from the Asian Mountains (GAMDAM) Glacier Inventory (Nuimura et al., 2015) and the Randolph Glacier Inventory version 4.0 (RGI; Arendt et al., 2014). For the glaciers lacking elevation information, we drop glacier outline over the ASTER GDEM2.0 (Tachikawa et al., 2011), then obtain the elevation information from the ASTER GDEM2.0. For the glaciers lacking length information, we calculate glacier length based on a relation between glacier length and maximum and minimum elevations from Hirabayashi et al. (2013).

For the discretization of the study area, we divide each glacier into a set of elevation bands at intervals of 50 m. To generate temperature and precipitation time series for each elevation band of a glacier as inputs to the model, we calculate the time series from the grid point of the WRF data set closest to the glacier according to the mean elevation of the band using altitude-dependent lapse rates. However, there is no information about the spatial variability of the temperature lapse rate and the precipitation vertical gradient in the Altai Mountains due to the lack of observed meteorological data sets in high-elevation regions. Here, we estimate these parameters at each glacier location through regressing the temperature and precipitation of  $4 \times 4$  WRF grid points around the glacier onto elevation, longitude, and latitude. This approach has been confirmed that it is useful for temperature and precipitation estimations at unsampled sites (e.g., Fang and Yoda, 1988; Marzeion et al., 2012; Li et al., 2013; Zhang et al., 2016).

#### 4.2. Mass balance model

Surface mass balance for each individual glacier in the Altai Mountains is calculated using a temperature index-based glacier mass-balance model. The model computes the major components of the glacier mass budget, including snow accumulation, snow and ice melt, and refreezing, and considers the feedback between the surface mass balance and changing glacier hypsometry. We run the model at daily temporal resolution for each 50 m elevation band of each individual glacier, and define the mass-balance year as the period from 1 October to 30 September of the following year. A detailed description of the model components is given in Hirabayashi et al. (2010) and Zhang et al. (2016).

In the present mass-balance model, snow accumulation for each elevation band is modelled from the precipitation value using a temperature threshold ( $2^\circ\text{C}$ ) to discriminate rain from snow. Precipitation is assumed to fall as snow at or below the threshold temperature, while it is assumed to be rain above the threshold temperature. A mixture of snow and rain is assumed within a transition zone ranging from 1 K above to 1 K below the threshold temperature. Within this temperature range, the snow and rain percentages of total precipitation are obtained by linear interpolation. Redistribution of snow by wind or avalanches is not considered in this study.

We calculate snow and ice melt for each elevation band through a temperature-index model that is based on an empirical relationship between melt and air temperature (Braithwaite and Zhang, 2000; Hock, 2003). For an elevation band ice melting occurs only if no snowpack remains in the band. The model differentiates between degree-day factors (DDFs) for ice and snow, which show significant variability from site to site (Hock, 2003; Zhang et al., 2006). To assign the DDFs for ice and snow to each individual glacier of the Altai Mountains, we use a set of empirical functions to estimate the DDFs for ice and snow. The empirical functions relate the observed DDFs for snow and ice on the forty glaciers in the Tibetan Plateau and surroundings to the climatic setting of each glacier (defined by annual temperature and precipitation from the WRF data set closest to the glacier), the mean glacier elevation, and the geophysical location from the glacier inventory (Zhang et al., 2017a). Overall, the DDFs for ice vary from 6.0 to

$11.0 \text{ mm d}^{-1} \text{ }^\circ\text{C}^{-1}$  with an average value of  $8.6 \text{ mm d}^{-1} \text{ }^\circ\text{C}^{-1}$ , and for snow vary from 1.5 to  $6.1 \text{ mm d}^{-1} \text{ }^\circ\text{C}^{-1}$  with an average value of  $4.1 \text{ mm d}^{-1} \text{ }^\circ\text{C}^{-1}$ .

Surface melting does not necessarily equate to mass loss for a glacier due to refreezing (Woodward et al., 1997; Fujita and Ageta, 2000; Wright et al., 2007). If melting occurs at the surface of a cold snowpack some of the surface meltwater will percolate into the snowpack and refreeze. To account for the impact of this process, we adopt a parameterized approach to estimate refreezing. Our approach follows that developed by Woodward et al. (1997). They proposed a relation between potential depth of meltwater refreezing and mean annual air temperature. Any snow melting from a given elevation band refreezes at depth in the snowpack until the potential depth of refreezing has been melt, after which additional meltwater runs off the glacier. A detailed description of the approach can be found in the study of Woodward et al. (1997). To capture the feedback between the surface mass balance and changing glacier hypsometry (i.e., changes in volume, surface area and elevation range), volume-area and volume-length scaling is used to adjust glacier volume and length after computing surface mass balance. This approach is based on a theoretical analysis of glacier dynamics and glacier geometry (Bahr et al., 1997; Bahr, 1997), which has been used widely to model changes in glacier hypsometry in different studies on different scales (e.g., Radić et al., 2008; Radić and Hock, 2010, 2011; Marzeion et al., 2012; Hirabayashi et al., 2013). The volume ( $V$ ) of a glacier is related to its surface area ( $A$ ) and its length ( $L$ ) via a power law:

$$V = c_a A^\gamma \quad (1)$$

$$V = c_l L^q \quad (2)$$

where  $c_a$ ,  $c_l$ ,  $\gamma$ , and  $q$  are scaling parameters, the values of which are  $0.2055 \text{ m}^{3-2\gamma}$  (Chen and Ohmura, 1990),  $1.7026 \text{ m}^{3-2\gamma}$  (Radić and Hock, 2010; Hirabayashi et al., 2013),  $1.375$  (Bahr et al., 1997), and  $2.0$  (Hirabayashi et al., 2013), respectively.

Initial glacier volume is estimated from glacier area using volume-area scaling. After the computation of surface mass balance, glacier area is updated, and thus volume changes after each time step. Furthermore, volume-length scaling is used to adjust glacier length when volume changes. The change in glacier length determines the elevation range of the glacier, which allows for removing or adding area along the entire length of the glacier (Radić et al., 2008). When glacier retreats, the area change is computed from the area-altitude distribution of the lost elevation bands, while in case of glacier advance, the length is allowed to increase assuming that the area-altitude distribution is kept unchanged. The area for each elevation band is calculated using a normal distribution derived from glacier area and the range between maximum and minimum elevation (Hirabayashi et al., 2010; Zhang et al., 2016). This approximation relies on the argument that the observed area-altitude distribution tends to have a normal distribution for the Altai glaciers (Fig. 2a).

#### 4.3. Model validation

Due to the sparsity of observational data in the Altai Mountains, validating our modelling approach to more than a thousand glaciers is challenging, but it is crucial for the model to realistically capture the governing processes of glacier mass budget. Therefore, we apply a multilayer procedure to cross-validate our modelling approach based on all available observed or previously estimated data sets in the study region. These data include: (1) observed annual mass balances for the five glaciers (Leviy Aktru, Maliy Aktru, Vodopadniy, Potanin and Tsambagarav glaciers); (2) geode-

tic mass changes of the fourteen glaciers in the Chinese Altai Mountains; and (3) area change rates of the eighteen glaciers in the Chinese Altai Mountains and the Aktru River Basin. Although the data series are generally short and partly discontinuous, the combination of in situ observations of surface mass balance, geodetic mass changes, and satellite-derived observations of glacier area changes allows us to draw an integrative validation of our modelling approach in the Altai Mountains.

In a first step, the model is validated against in situ measurements of annual mass balances on Levij Aktru, Maliy Aktru, Vodopadniy, Potanin and Tsambagarav glaciers. This allows evaluating the ability of the model to reproduce annual mass balance variability. Then, our model results are compared to geodetic mass changes of the fourteen glaciers in the Chinese Altai Mountains for the period 1999–2008, which are fully independent from our results. Finally, we use satellite-derived area changes of the eighteen glaciers in the Aktru River Basin for the period 1999–2008 and the Chinese Altai for the period 2000–2008 to validate the predictive capability for capturing the feedback between the surface mass balance and changing glacier hypsometry.

Two assessment criteria are used to evaluate the model performance, which are the correlation coefficient ( $r$ ) and the mean absolute error (MAE) between observed and modelled balance. The correlation coefficient provides an indication of the ability of the model to capture the mass balance variation, while the MAE captures the model's ability to match the magnitude of the surface mass balance, indicating how well the model reproduces surface mass balance. The MAE is preferred to the commonly used root mean square error because MAE provides a more robust indicator of the sizes of errors.

## 5. Results

### 5.1. Model performance

We first evaluate the WRF outputs against observations at ten weather stations over the Altai Mountains. Unless otherwise stated, all significance levels of correlation coefficients ( $r$ ) presented herein are  $p < 0.001$ . Daily, monthly and annual WRF temperature and precipitation means correlate well with ground observations averaged from ten weather stations for the period 1990–2011 (Fig. 3). Analysis of the daily, monthly, and annual temperature data yields correlation coefficients ( $r$ ) of 0.98, 0.99 and 0.88, and MAEs of 2.0, 1.2 and 0.1 °C (Fig. 3a, c and e), respectively. As expected, the correlations for precipitation are lower than those for temperature (Fig. 3). Analysis of the daily, monthly, and annual precipitation data yields correlation coefficients ( $r$ ) of 0.63, 0.77 and 0.71, and MAEs of 0.8, 0.4 and 0.2 mm d<sup>-1</sup> (Fig. 3b, d and f), respectively. Seasonally, the correlations between the observed and WRF temperatures are 0.94, 0.88, 0.92 and 0.82 for the spring (March, April, May (MAM)), summer (June, July, August (JJA)), autumn (September, October, November (SON)), and winter (December, January, February (DJF)), respectively, and the MAEs are 2.5, 0.3, 0.6 and 0.8 °C. This implies that the WRF temperature is able to capture the observed seasonal variability well (Fig. 4a). The seasonal temporal trend in temperature during 1990–2011 estimated from the weather stations and the WRF simulation is presented in Fig. 4a. We find good agreement for the seasonal temporal trend between ground observations and WRF simulations. With the exception of the winter experiencing the decreasing trend in temperature, the increasing trend occurs in other seasons (Fig. 4a). Similar to temperature, the observed seasonal variability in precipitation is captured well (Fig. 4b). The correlations between the observed and WRF precipitation are 0.73, 0.61, 0.70 and 0.88 for the spring, summer, autumn, and winter, respectively, and

the MAEs are 0.5, 0.6, 0.4 and 0.6 mm d<sup>-1</sup>. Moreover, the temporal trend of the WRF precipitation matches the observation well (Fig. 4b). The largest increasing trend occurs in March, while the significant decreasing trend occurs in July and September.

While the observed seasonal variability in precipitation is well captured, the WRF model overestimates the precipitation compared to ground observations (Fig. 4b). Similar results showing an overestimation in precipitation have been found over the Tibetan Plateau (Gao et al., 2015). It is well known that there is no optimal model strategy of precipitation applicable for high-mountain regions due to extremely complex topography. Although the problem of the orographic bias remains unsolved in high-elevation regions, the WRF model has been confirmed its good accuracy in simulating snow- and rainfall on the Tibetan Plateau and surroundings (Maussion et al., 2011; Collier et al., 2013; Gao et al., 2015). In high-elevation regions of the Altai Mountains, validation studies of the WRF outputs were carried out (Kitabata et al., 2014; Sugiura et al., 2014). The daily temperature, accumulated precipitation amount, and snow water equivalent (SWE) simulated by the WRF model were compared to the Global Surface Summary of the Day product provided by the National Climate Data Center (NCDC), in situ observations of summer precipitation in 2006 in different high-elevation sites, and snow surveys from the Mongolian Altai Mountains of >2000 m a.s.l. in 2008. This comparison confirmed that the WRF model can accurately simulate the surface temperature, precipitation, and SWE in high-elevation regions of the Altai Mountains, especially for the elevation dependency and seasonality of precipitation and SWE in the presence of spatial variability (Kitabata et al., 2014; Sugiura et al., 2014). Overall, the above analyses suggest that the WRF temperature and precipitation data used in this study correspond sufficiently well with ground observations, which can be used as input for the mass balance model in the Altai Mountains.

To validate the model performance, we run our modelling approach to calculate the surface mass balance of each of the five glaciers over the corresponding observation period (Table 1). Altogether, a total set of 72 pairs of modelled and observed annual mass balances is obtained. A scatter diagram of modelled and observed mass balances of the five glaciers is presented in Fig. 5a, along with the observed and modelled time series of annual mass balance in the Aktru River Basin (Fig. 5b). We find a good agreement between the modelled and observed annual mass balances of the five glaciers. The correlation coefficient ( $r$ ) between simulations and observations is 0.80, and the overall MAE is 0.23 m w.e. The long-term variation in glacier mass balance of the Aktru River Basin indicates that our modelling approach slightly overestimates the magnitude of negative mass balances in some years (Fig. 5b). This can be attributed to the limited skill of the estimated the DDFs for ice and snow to reproduce year-to-year mass balance variability. However, most observed annual mass balance time series fall within one standard deviation of the estimated annual mass balance, which demonstrates that our modelling approach is able to capture much of the observed temporal variability (Fig. 5b).

Moreover, we validate model results against satellite-based mass change rates on the fourteen glaciers in the Chinese Altai Mountains. The satellite-based observations are fully independent from our model results. A comparison between the modelled results and the satellite-based mass change rates of these glaciers indicates that the results from the two independent approaches agree well (Fig. 5b). It yields  $r = 0.82$  and MAE = 0.20 m w.e. yr<sup>-1</sup>. The satisfying agreement with geodetic approach allows us to use our model to calculate annual surface mass balance on individual glaciers for a longer time period.

In addition, reduction rates in area of the four glaciers in the Aktru River Basin and the fourteen glaciers in the Chinese Altai Mountains were obtained from satellite data, respectively, during

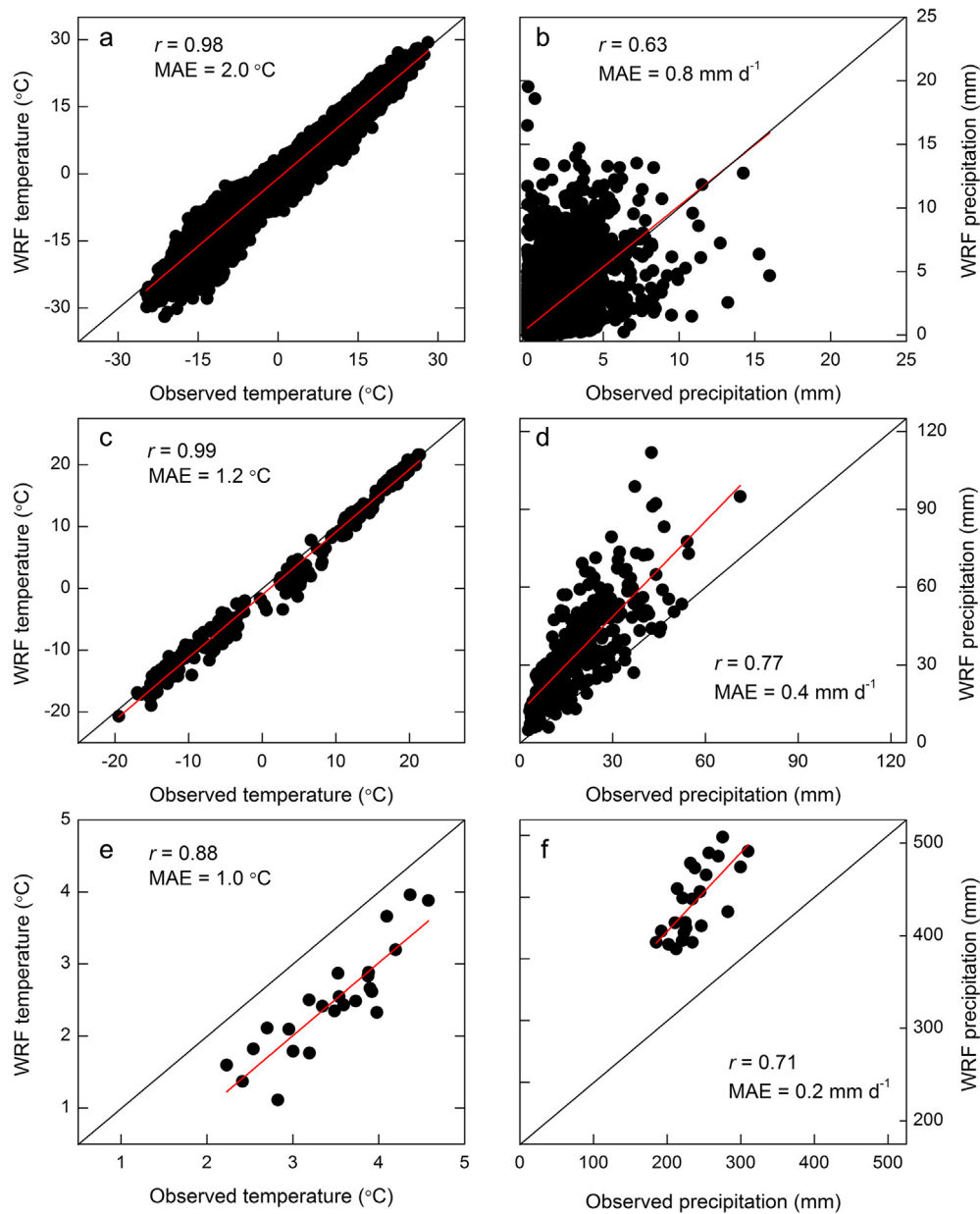


Fig. 3. Scatter plots of daily (a and b), monthly (c and d), and annual (e and f) temperature and precipitation between the WRF simulation and station observation.

1999–2008 (Narozhniy and Zemtsov, 2011) and during 2000–2008 (Wei et al., 2015). For each of these glaciers, our model simulates its surface area for the years of satellite-based observations. A comparison of the modelled results and satellite-based observations indicates that our modelling approach provides good results for periods of glacier area change (Fig. 5d), yielding the  $r$  value of 0.83 and the MAE value of  $0.015 \text{ km}^2 \text{ yr}^{-1}$ . This implies that the approach is capable of capturing the feedback between glacier mass balance and change in glacier area.

As discussed above, our model generally reproduces the observations and the previous estimations well, explaining a large proportion of the variability in the annual mass balance. In particular, the two independent approaches show a satisfying agreement, indicating the capability of the model for simulating mass balance variation and changes in glacier area in the study region. This gives us confidence to use the model to extend the estimates on individual glaciers over a considerably longer time period and to obtain insights in differences from site to site.

## 5.2. Mass balance since 1990

The time series of the modelled annual specific mass balance for the entire Altai Mountains is depicted in Fig. 6a. The results reveal an average annual glacier mass balance rate of  $-0.69 \text{ m.w.e. yr}^{-1}$  over the period 1990–2011. Compared with the mass loss rate estimated in other regions, the mass loss rate of the study region is slightly larger than those of the Tien Shan ( $-0.45 \text{ m.w.e. yr}^{-1}$  over the period 1971–2009; Liu and Liu, 2015) and the Suntar-Khayata Range ( $-0.52 \text{ m.w.e. yr}^{-1}$  over the period 1991–2014; Zhang et al., 2017b). This implies that the Altai Mountains show marked mass loss in the Northern part of Asia.

Although three positive balance years occur within the 22-year period (1990–2011), mass loss rates have grown progressively for the whole region since 1990 (Fig. 6a). We detect two periods of rapid mass loss over the 22-year period, which are 1996–2000 and 2007–2011 (Fig. 6a). The mean annual mass balance of the two periods is about  $-1.1 \text{ m.w.e.}$  for the whole region. Although

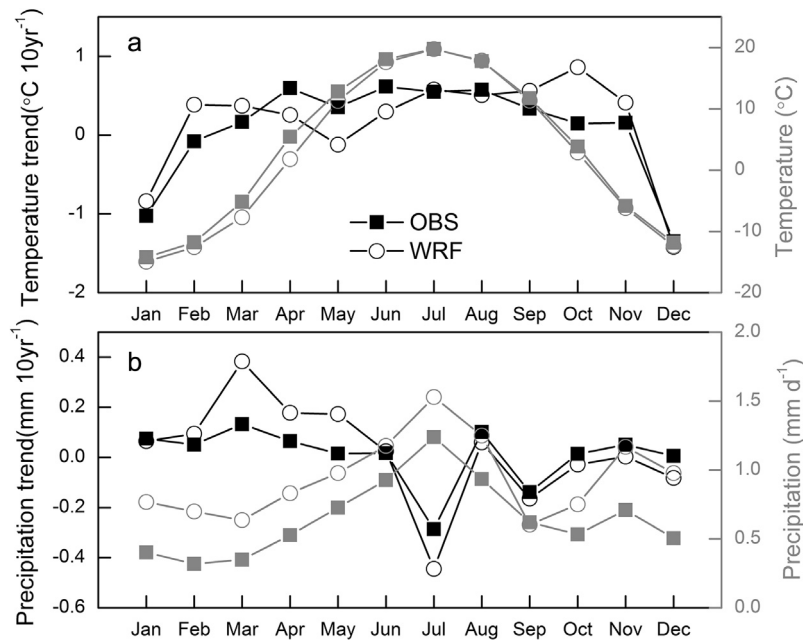


**Fig. 4.** Seasonal temporal trend (black) and seasonal variation (grey) of temperature (a) and precipitation (b) during 1990–2011 estimated from ten weather stations (OBS) and the WRF simulations (WRF).

one positive mass balance year occurs during 2007–2011, the mass loss rate is approximately two times as much as the mean value over the period 1990–2006. Such an accelerated mass loss is confirmed by observed mass balances on different glaciers (Fig. 6b). Observations in the Aktru River Basin indicate that glaciers of the basin are dominated by the positive mass balance before 1990, while negative mass balances become dominant after 1990 (Fig. 6b). The mean specific mass balance of the Aktru River Basin is about +0.01 m w.e. for the period 1977–1990, whereas it is about -0.23 m w.e. for the period 1991–2011. Specifically, observations on the glaciers of the Aktru River Basin suggest a dramatic decrease in ice mass with a rate of  $-0.42 \text{ m w.e. yr}^{-1}$  in recent years (2007–2011). Such a trend is also observed on the Potanin and Tsambagarav glaciers (Fig. 6b), where the mass loss rates are  $-0.84$  and  $-0.99 \text{ m w.e. yr}^{-1}$ , respectively, during 2008–2011. For the entire study period, the cumulative mass balance of the whole region is about  $-15.2 \text{ m w.e.}$  for the period 1990–2011 (Fig. 6a), about 35% of which is observed during 2007–2011.

The spatial variability of the surface mass balance for the Altai glaciers is shown in Fig. 7. Of all Altai glaciers, about 81.3% experience considerable mass loss, representing approximately 78% of the total glacier area. We find marked differences in the rate of mass change from site to site for the period 1990–2011 (Fig. 7). The highest mass-loss rates are found in the Katun Ridge and western parts of the Chuya Ridge and Tavan Bogd Range during the entire period (specific mass-loss rate:  $-1.1 \text{ m w.e. yr}^{-1}$ ). Tsambagarav and Kharkhiraa massifs are characterized by a relatively moderate mass loss over the past 22 years ( $-0.77 \text{ m w.e. yr}^{-1}$ ). Comparable low mass-loss rates or slight mass gain are found in the eastern parts of the Chuya Ridge and Tavan Bogd Range and the southeastern part of the Mongolian Altai Mountains ( $-0.1 \text{ m w.e. yr}^{-1}$ ).

For different size classes, glaciers for the size class of  $0.1\text{--}0.5 \text{ km}^2$  dominate in the region in terms of the total number (Fig. 2b). These glaciers experience the most considerable mass loss in the region over the past 22 years, with a mass loss rate of  $-0.98 \text{ m w.e. yr}^{-1}$ . Glaciers for the size class of  $1.0\text{--}5.0 \text{ km}^2$  dominate in terms of the total area (Fig. 2b), the average mass-loss rate

of which is similar to that of the whole region (Fig. 2c). Note that the glaciers for the size class of larger than  $10.0 \text{ km}^2$ , representing 12.0% of the total glacier area, experiences the smallest mass loss in the region (Fig. 2c).

### 5.3. Influence of glacier mass change on water resources and sea-level change

The majority of glaciers in the Altai Mountains have experienced considerable shrinkage during the past decades (Kadota and Gombo, 2007; Surazakov et al., 2007; Shahgedanova et al., 2010; Kadota et al., 2011; Narozhniy and Zemtsov, 2011; Yao et al., 2012; Krumwiede et al., 2014; Syromyatina et al., 2015; Wei et al., 2015), and accelerated mass loss trend is found during recent years (Fig. 6). Accelerated glacier wastage in the region is a potential impact on regional water availability. Such issue becomes of particular concern due to the local demand water increasing with the local population growth (Lutz et al., 2014; Pritchard, 2017), rapid urbanization and economic development (Priess et al., 2011) and the continued glacier shrinkage anticipated in response to climatic changes.

For the period 1990–2011 and the entire Altai Mountains, the results indicate a total meltwater discharge from glaciers of  $401.1 \times 10^8 \text{ m}^3$ . This amount is about four times as much as the average annual discharge of the Irtysh River Basin in China (Li et al., 2010). Such a loss of glacial meltwater is of vital significance to water resources in the Altai Mountains, especially in the semi-arid and arid regions where the water supply is extremely limited. In the Mongolia, about 10.8% of the total water resources is stored in glaciers, which is the second source of freshwater within this region, besides lakes (Pan, 2013). Our estimates indicate that in addition to Tsambagarav and Kharkhiraa massifs characterized by a relatively moderate mass loss over the past 22 years, other regions experience comparable low mass-loss rates or slight mass gain in the Mongolian Altai Mountains (Fig. 7). This implies that in combination with a positive change in precipitation (Fig. 8), such low glacier mass-loss rate may not be a potential threat to human populations through impacts on water availability, and will con-

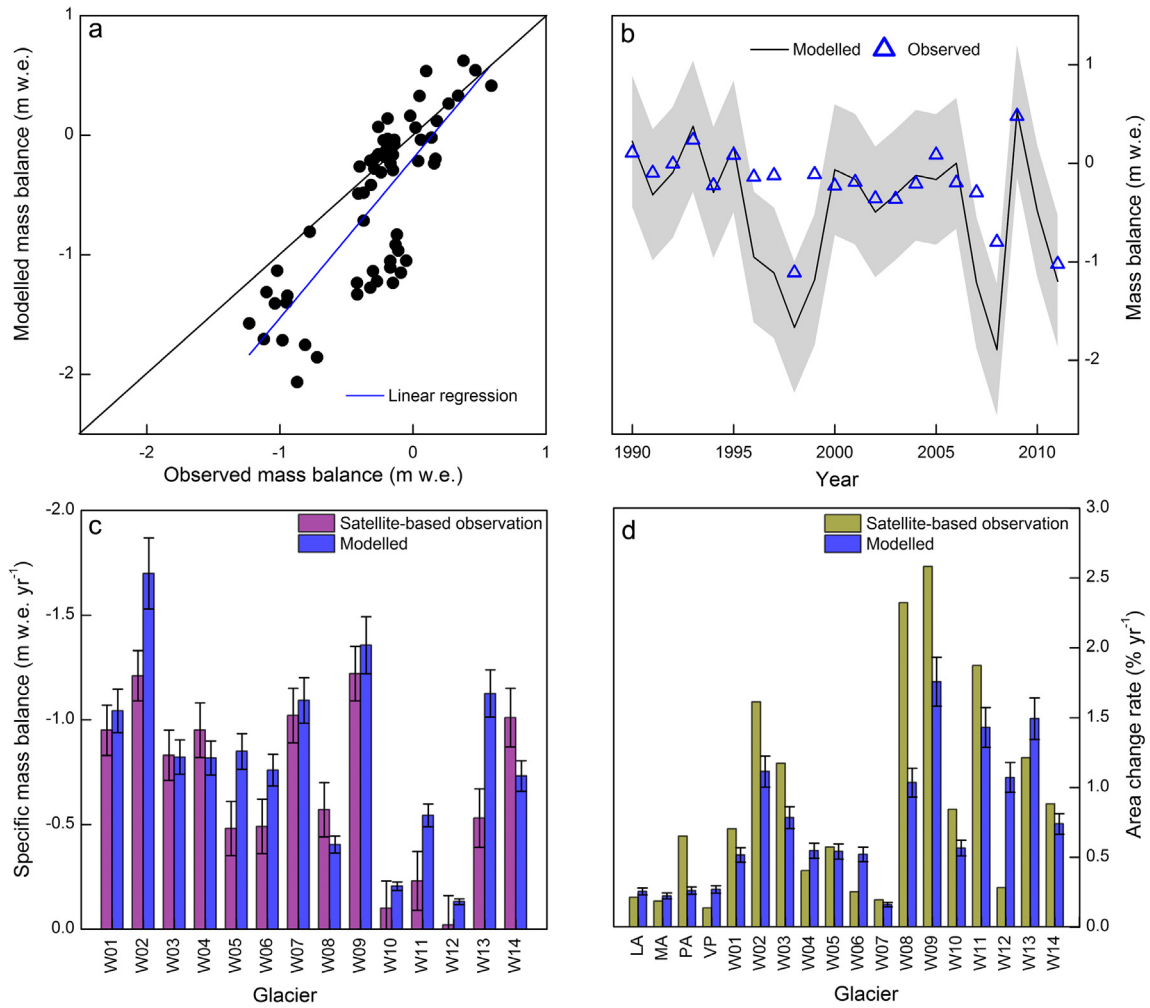


**Fig. 5.** (a) Scatter diagram of observed and modelled annual mass balance for the corresponding observation period, (b) time series of observed and modelled annual mass balance in the Aktru River Basin over the period 1990–2011, (c) geodetic mass change rates and modelled results on the fourteen glaciers in the Chinese Altai Mountains, and (d) satellite-based observed and modelled glacier area change in the Aktru River Basin over the period 1999–2008 and the Chinese Altai Mountains over the period 2000–2008. Light gray shading in (b) denotes the standard deviation of the estimated mass balance, and error bar in (c and d) indicates standard error. LA, MA, PA and VP denote the four glaciers in the Aktru River Basin and W01–W14 denote the fourteen glaciers in the Chinese Altai Mountains and their information can be found in [Wei et al. \(2015\)](#).

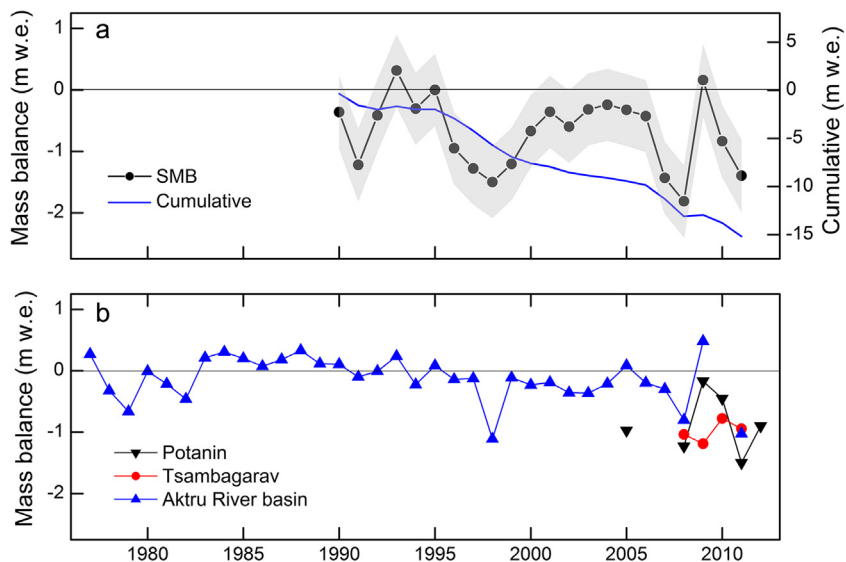


**Fig. 6.** (a) Time series of the modelled annual and cumulative mass balance of the entire glaciers in the Altai Mountains during 1990–2011, and (b) observed annual mass balance of different glaciers during 1977–2012. Light gray shading in (a) denotes the standard deviation of the estimated mass balance.

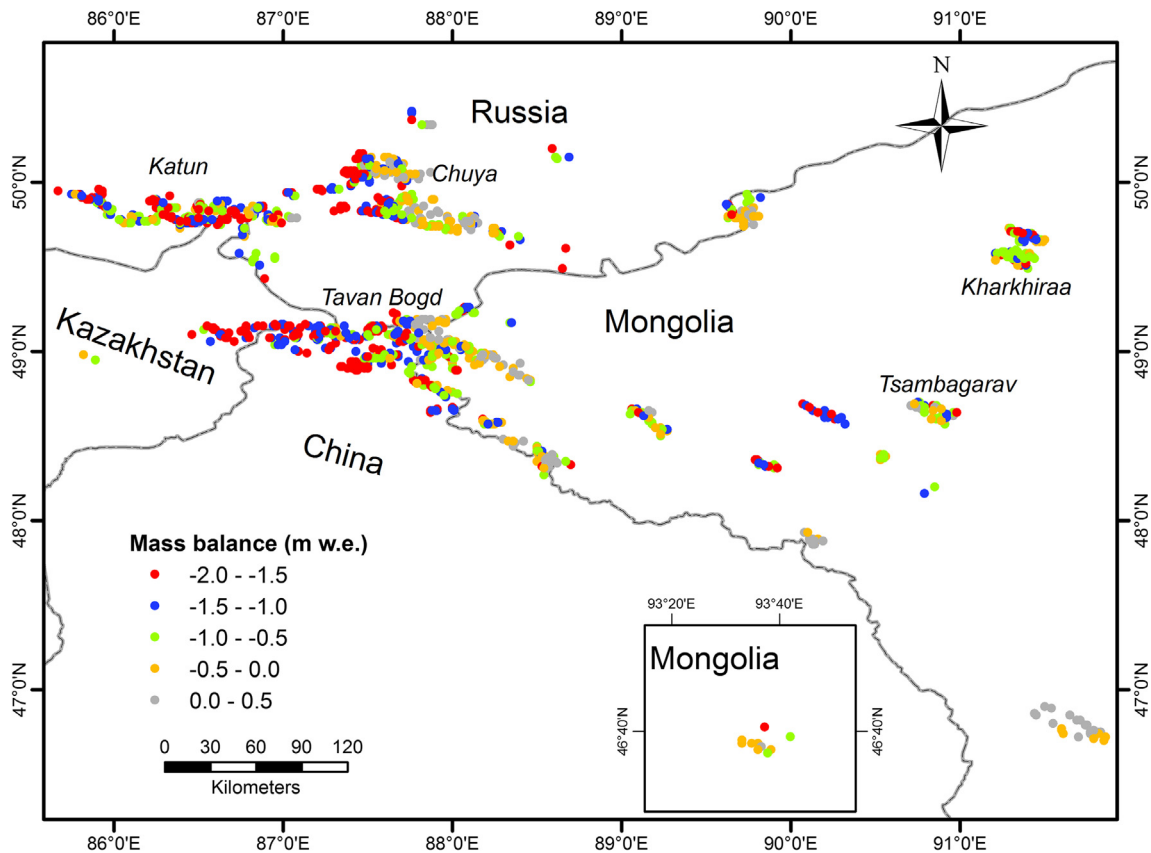


Fig. 7. Spatial variability of modelled surface mass balance of the glaciers in the Altai Mountains averaged during 1990–2011. The bottom right shows glacier mass balance in the southeastern part of the Mongolian Altai Mountains.

tinue to sustain the increasing water demands expected in the Mongolia. Furthermore, the meltwater discharge significantly increases in recent years, accompanied by a significant decrease in glacier area and mass. On average, glaciers in the study region provide an extra  $7.1 \times 10^8 \text{ m}^3$  of meltwater annually for the period 2007–2011 compared to that for the period 1990–2006, about 7.1% of average annual discharge of the Irtysh River basin in China. This implies that to a certain extent, the influence of glacier mass change on water resources has become stronger than ever before in the Altai Mountains.

For sea-level change calculations, we simply convert the rate of glacier net mass loss into sea-level equivalent by dividing the volume of water lost by the ocean area ( $362.5 \times 10^{12} \text{ m}^2$ ), thus neglecting the effects of altering ocean area and terrestrial hydrology. According to our results and previous estimates (Dyurgerov, 2010; Radić and Hock, 2011), we find that the contribution to sea-level rise from the glaciers of the Altai Mountains has grown during the past decades (Fig. 9). For the period 1961–2006 the contribution to sea-level rise is only  $0.0005 \text{ mm yr}^{-1}$ , whereas it is  $0.0010 \text{ mm yr}^{-1}$  during 1993–2006 (Dyurgerov, 2010). During recent years (2007–2011) the contribution to sea-level rise from the entire glaciers is about  $0.0023 \text{ mm yr}^{-1}$ , more than four times as much as that during 1961–2006 (Dyurgerov, 2010).

## 6. Discussion

### 6.1. Climate change and glacier mass change

The glacier mass changes in the Altai Mountains for the period 1990–2011 are characterized by significant sub-regional differences (Fig. 7). Note that climate forcing is a major external control

on the mass change of a glacier (Cuffey and Paterson, 2010). An overview of mean annual temperature and precipitation and their changes for the period 1990–2011 calculated from WRF data sets is presented in Fig. 8. The distinct patterns of mean annual air temperature and annual precipitation are clearly detectable, that is, the climatic environment of the region varies gradually from cold and dry conditions of the southeast to warm and wet conditions of the northwest (Fig. 8a and c). The air temperature has increased significantly during the study period over the Altai Mountains (Fig. 8b), with warming rates varying from 0.02 to  $0.25 \text{ }^\circ\text{C} (10 \text{ yr})^{-1}$  as calculated by a linear trend. This trend coincides with the findings suggested by instrumental records in the Chuya Ridge (Surazakov et al., 2007; Shahgedanova et al., 2010; Narozhniy and Zemtsov, 2011) and the Chinese Altai Mountains (Yao et al., 2012) and reconstructions of past climate from the ice cores drilled in Belukha Glacier (Henderson et al., 2006; Okamoto et al., 2011). The warming rates for most glaciers over the 22 years are larger than the global warming rate calculated during 1951–2012 (Hartmann et al., 2013). For the entire region, previous studies found a decrease in precipitation since the 1980s (Kitabata et al., 2014; Malygina et al., 2017), and an accelerated decrease trend is especially observed since the year 2000 (Kitabata et al., 2014). Wei et al. (2015) suggested that the annual precipitation in the Chinese Altai Mountains decreases by 4–8 mm during the period 1999–2008. As shown in Fig. 8d, precipitation change over the region is relatively complicated with rates varying from  $-7.0$  to  $+8.0 \text{ mm yr}^{-1}$ .

To assess the relationship between the glaciers and climate change, mass balance sensitivities to changes in air temperature and precipitation are often used (Oerlemans and Fortuin, 1992; Braithwaite et al., 2002; Radić and Hock, 2011). For all Altai gla-

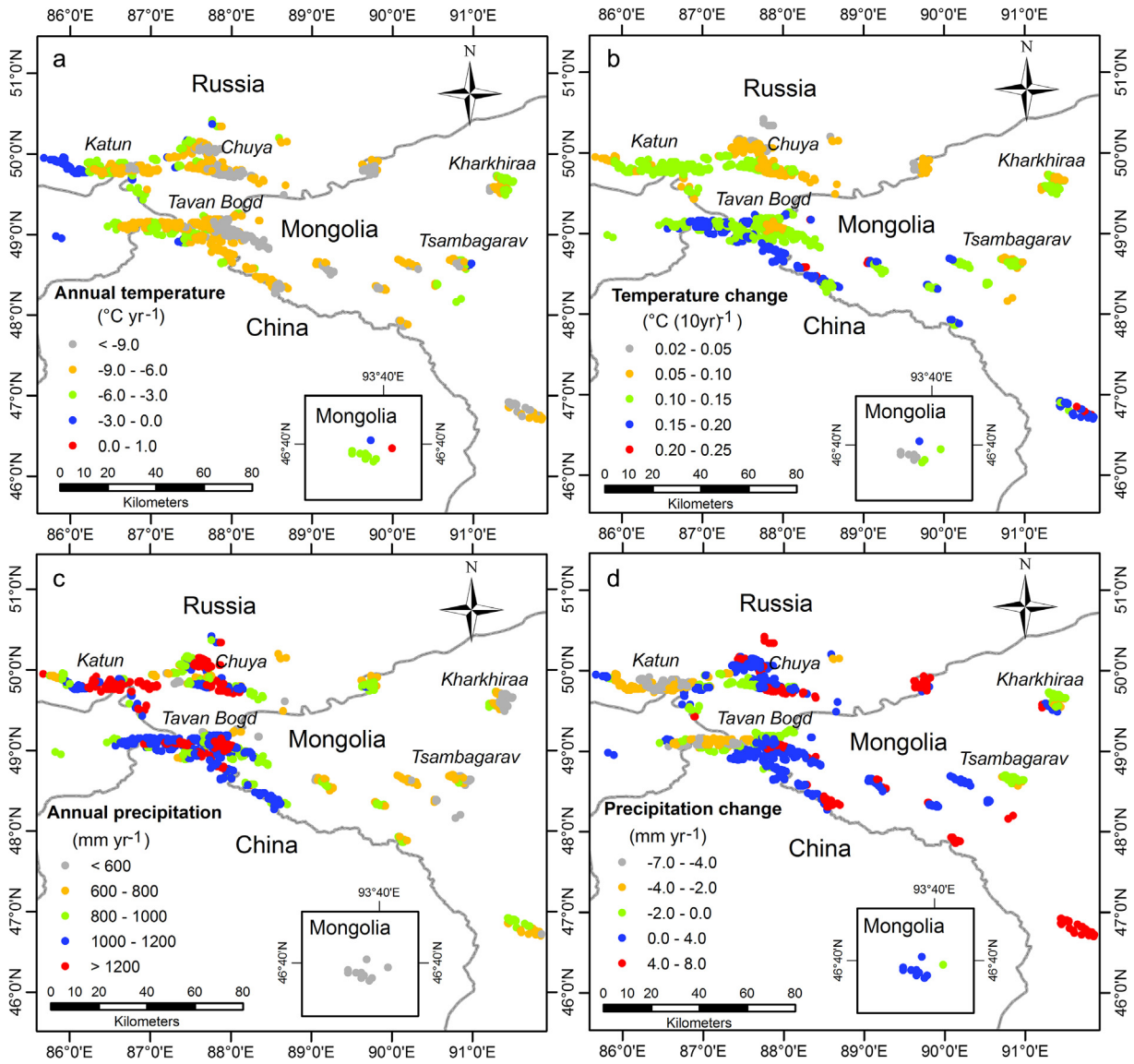


**Fig. 8.** Spatial patterns of mean annual air temperature (a), trend in temperature change (b), annual precipitation (c), and trend in precipitation change (d) over the period 1990–2011 on each glacier in the Altai Mountains calculated from WRF data. The bottom right in each figures shows the spatial patterns on each glacier in the southeastern part of the Mongolian Altai Mountains.

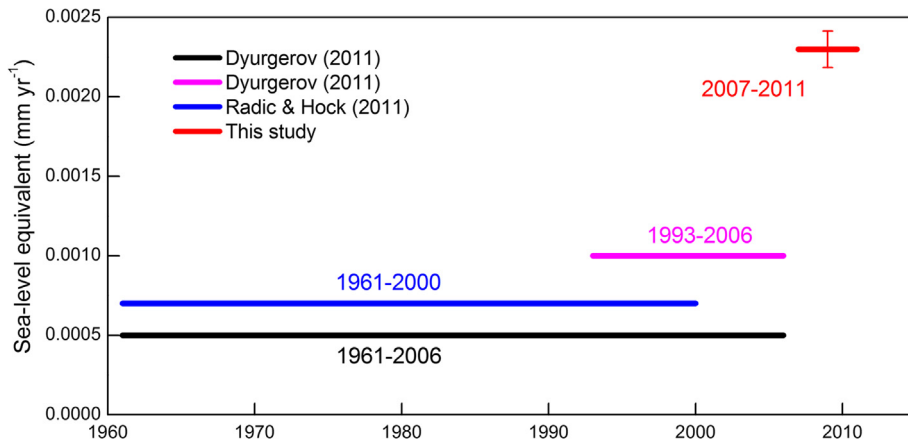


**Fig. 9.** Contribution to sea-level rise from the entire glaciers of the Altai Mountains during different periods.

ciers, we calculate mass balance sensitivities to an air temperature rise of 1 °C ( $\Delta\bar{B}/\Delta T$ ) and a change in precipitation of +10% ( $\Delta\bar{B}/\Delta P$ ). The results indicate that the average mass balance sensitivities to a +1 °C rise in temperature and a 10% increase in precipitation are about  $-0.56 \text{ m w.e. yr}^{-1} \text{ } ^\circ\text{C}^{-1}$  and  $+0.11 \text{ m w.e. yr}^{-1} (10\%)^{-1}$ , respectively, for the whole Altai Mountains. The average  $\Delta\bar{B}/\Delta T$  agrees well with that estimated by Radić and Hock (2011), and is slightly higher than a global sensitivity of  $-0.4 \text{ m w.e. yr}^{-1} \text{ } ^\circ\text{C}^{-1}$  (Oerlemans and Fortuin, 1992). Compared with the  $\Delta\bar{B}/\Delta T$  estimated in other regions, we find that the  $\Delta\bar{B}/\Delta T$  of the study region is similar to those of the Tibet, Tien Shan and Suntar-Khayata Range (Radić and Hock, 2011), and is smaller than those of Iceland, Scandinavia and Alps (Braithwaite et al., 2002; Radić and Hock, 2011). The average  $\Delta\bar{B}/\Delta P$  of the region is slightly higher than that estimated by Radić and Hock (2011);  $-0.07 \text{ m w.e. yr}^{-1} (10\%)^{-1}$ . This value is slightly larger than those of its surroundings, such as the Suntar-Khayata Range, Tien Shan and Pamir (Radić and Hock, 2011), and is smaller than those of Iceland, Scandinavia and Alps (Braithwaite et al., 2002; Radić and Hock, 2011). In addition, an experiment is made by involving changes in precipitation as well as temperature. We find that increased precipitation would partly offset the effect of higher temperature, but a 10% increase in precipitation cannot compensate for the increased ablation due to a 1 °C temperature rise.

Fig. 10 shows the spatial variability of  $\Delta\bar{B}/\Delta T$  and  $\Delta\bar{B}/\Delta P$  for individual glaciers of the Altai Mountains. Temperature sensitivities for individual glaciers show a strong variability, which are between  $-0.05$  to  $-1.38 \text{ m w.e. yr}^{-1} \text{ } ^\circ\text{C}^{-1}$ , whereas precipitation sensitivities vary from  $+0.03$  to  $+0.23 \text{ m w.e. yr}^{-1} (10\%)^{-1}$ . The majority of glaciers in the western part of the region have statistically significant  $\Delta\bar{B}/\Delta T$  and  $\Delta\bar{B}/\Delta P$ , which are largely higher than those in the eastern part of the region. In particular, glaciers in the Mongolian Altai Mountains show the lowest sensitivities to temperature and precipitation changes compared to other regions. Such spatial characteristics of  $\Delta\bar{B}/\Delta T$  and  $\Delta\bar{B}/\Delta P$  are mainly related with the climate conditions, i.e. the western part of the study region is much wetter than its eastern part (Fig. 8c). This demonstrates that the glaciers in wetter climate conditions are more sensitive to climate change compared to those in drier climate conditions. For different size classes, temperature sensitivities of the glaciers significantly varied are found (Fig. 2c), which are from  $-0.48$  to  $-0.73 \text{ m w.e. yr}^{-1} \text{ } ^\circ\text{C}^{-1}$ . Small glaciers for the size classes of  $<0.1$  and  $0.1\text{--}0.5 \text{ km}^2$ , which are dominant in the region in the light of the total number (Fig. 2b), show the higher sensitivity to temperature change (Fig. 2c). On the other hand, precipitation sensitivities of the glaciers for different size classes show the slight variability (Fig. 2c), which are between  $+0.10$  and  $+0.13 \text{ m w.e. yr}^{-1} (10\%)^{-1}$ .

The majority of glacier locations in the Katun Ridge, the western parts of the Chuya Ridge and Tavan Bogd Range, and Tsambagarav and Kharkhira massifs have experienced a decrease in precipitation over the past 22 years (Fig. 8d); meanwhile, an increase in air temperature is observed in these regions (Fig. 8b). The mass balance sensitivity experiments mentioned above indicate that the glaciers in these regions are more sensitive to temperature and precipitation changes (Fig. 10). Consequently, these glaciers have experienced considerable mass loss for the period 1990–2011 (Fig. 7). Other regions of the Altai Mountains, such as the eastern parts of the Chuya Ridge and Tavan Bogd Range and the southeastern part of the region, have experienced increasing both temperature and precipitation (Fig. 8). Although precipitation increases

(Fig. 8d), the limited change in precipitation is not sufficient to compensate for the increased melting due to temperature rise. This is confirmed by our experiment, which is made by involving

changes in precipitation as well as temperature, and reveals that a 10% increase in precipitation cannot compensate for the increased melting due to a 1 °C temperature rise. As a result, glaciers in these regions experience slight mass loss. Our finding is consistent with the detailed analysis of the links between glacier area changes of these regions and observed meteorological temperature and precipitation in previous studies (e.g., Surazakov et al., 2007; Shahgedanova et al., 2010; Narozhniy and Zemtsov, 2011; Yao et al., 2012), all of which suggest that glacier shrinkage is caused primarily by an increase in air temperature, although an increase in precipitation is observed.

## 6.2. Model parameters and uncertainty

For regional glacier mass balance modelling, part of the difficulty arises from the determinations of model parameters. In this study, temperature lapse rate ( $\gamma_{temp}$ ), precipitation gradient ( $\gamma_{precip}$ ) and the DDFs for snow and ice are mainly required parameters for our modelling approach. The DDFs for ice and snow can be computed from direct measurements for a glacier (e.g., Hock, 2003; Zhang et al., 2006) or calibrated based on mass balance observations for a large scale (e.g., Hirabayashi et al., 2010; Radić and Hock, 2011). In contrast, temperature lapse rate and precipitation gradient are difficult to estimate in high-elevation glacierized regions due to the lack of available temperature and precipitation data and their large spatial variability. The performance of glacier mass-balance models relies to a large degree on the data used to force the models in different elevations (Petersen and Pellicciotti, 2011; Immerzeel et al., 2014). In general, a constant free air lapse rate for temperature is used, which is often assumed to be the moist adiabatic lapse rate ( $-0.65 \text{ } ^\circ\text{C} (100 \text{ m})^{-1}$ ), whereas precipitation vertical gradient is more complicated.

To quantify the importance of these parameters for modelling mass balance, we rerun our modelling approach for all glaciers of the region using the six runs listed in Table 3. Runs 1–3 are to examine the impact of  $\gamma_{temp}$  and  $\gamma_{precip}$ , and runs 4–6 are to assess the impact of the DDFs for snow and ice. In runs 1 and 2, temperature lapse rate and precipitation gradient are considered to be constant values of  $-0.7 \text{ } ^\circ\text{C} (100 \text{ m})^{-1}$  and  $9.0\% (100 \text{ m})^{-1}$  (Table 3), respectively, which are the average values of the region, and other parameters remain the same as for the reference run in which these parameters are estimated as mentioned earlier. The result indicates that the rates of the regional mass balance estimated in runs 1 and 2 become less negative compared to the reference run, changes of which are about 11.1% and 7.3% (Table 3), respectively. In runs 4 and 5 the DDFs for snow and ice are considered to be constant values of 4.1 and 8.6  $\text{mm day}^{-1} \text{ } ^\circ\text{C}^{-1}$  (Table 3), respectively, which are the average values of the region, and other parameters remain the same as for the reference run. As a result, similar to runs 1 and 2, the rates of the regional mass balance estimated in runs 4 and 5 slightly change relative to the reference run (Table 3). Concerning run 3, both the lapse rates of temperature and precipitation are constant in space, whereas the DDFs for snow and ice are constant in run 6. Run 3 results in a significant change in the rate of regional mass balance with respect to the reference run, whereas run 6 leads to a slight change in the rate of regional mass balance (Table 3). These results indicate the high importance of spatial variability in these model parameters for the mass balance modelling. In particular, the spatial variability in temperature lapse rate and precipitation gradient plays an important role in these simulations on the regional scale.

Most modelling studies involve a calibration procedure, in which the model parameters are adjusted to yield maximum agreement between modelled and observed data. This process is a compromise between the methodological requirements for an

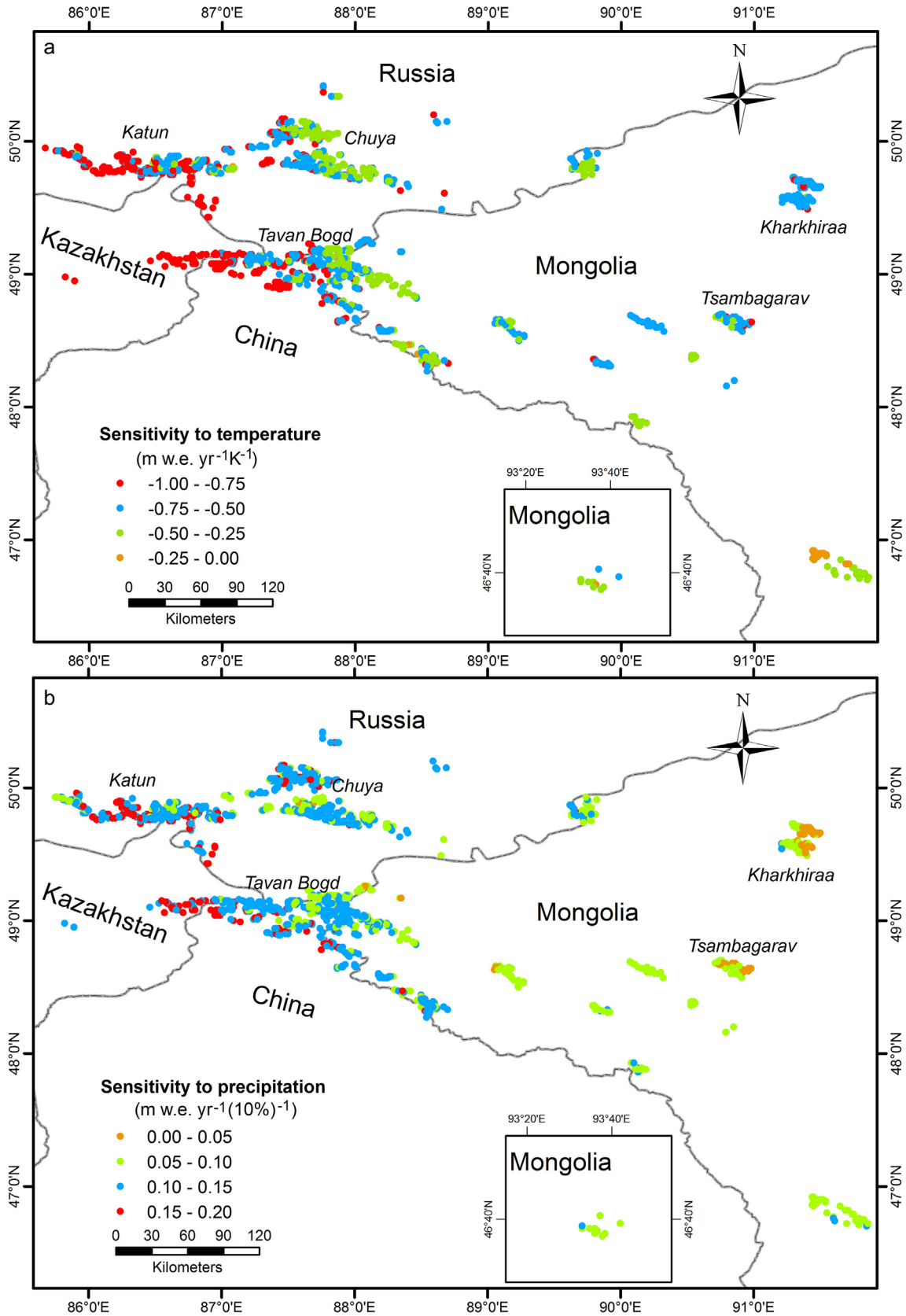


**Fig. 10.** Spatial variability of mass balance sensitivities of the entire glaciers to changes in (a) temperature and (b) precipitation in the Altai Mountains. The bottom right in (a) and (b) shows temperature and precipitation sensitivities in the southeastern part of the Mongolian Altai Mountains.

**Table 3**

Mass balance simulation experiment for different parameters required in the glacier mass-balance model. These parameters include temperature lapse rate ( $\gamma_{temp}$ ;  $^{\circ}\text{C} (100 \text{ m})^{-1}$ ), precipitation vertical gradient ( $\gamma_{precip}$ ;  $\% (100 \text{ m})^{-1}$ ) and DDFs for snow ( $ddf_{snow}$ ) and ice ( $ddf_{ice}$ ;  $\text{mm day}^{-1} \text{ }^{\circ}\text{C}^{-1}$ ). Reference run is the simulation using estimated parameters in the study.

Model run	Parameter constant	Values	Mass balance	Change (%)
Reference run	–	–	–0.690	–
Run 1	$\gamma_{temp}$	–0.70	–0.610	11.1
Run 2	$\gamma_{precip}$	9.0	–0.640	7.3
Run 3	$\gamma_{temp}$ and $\gamma_{precip}$	–0.70 and 9.0	–0.560	18.6
Run 4	$ddf_{snow}$	4.1	–0.659	4.5
Run 5	$ddf_{ice}$	8.6	–0.664	3.8
Run 6	$ddf_{snow}$ and $ddf_{ice}$	4.1 and 8.6	–0.662	4.0

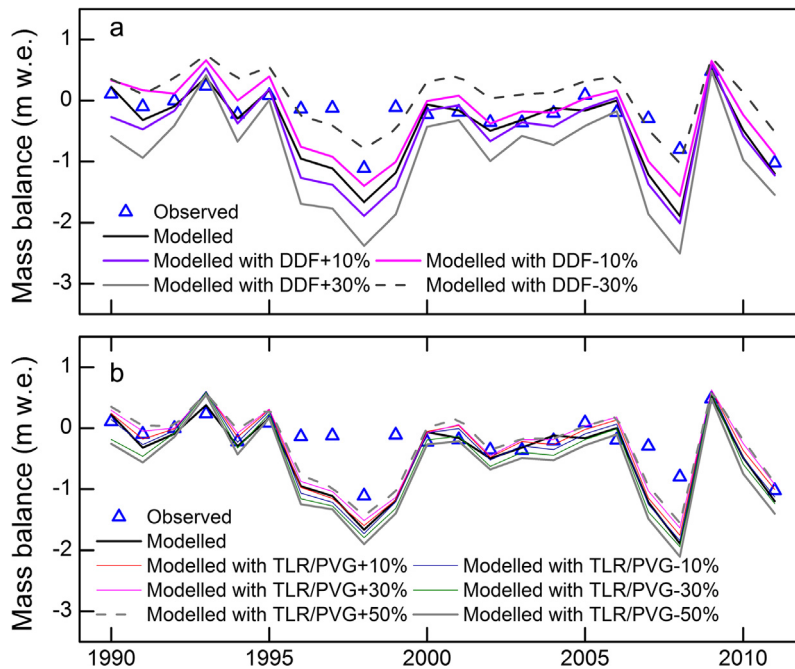


**Fig. 11.** Influences of changing in (a) the DDFs for snow and ice and (b) temperature lapse rates and precipitation gradients on modelling mass balance in the Aktru River Basin. Here, the DDFs for snow and ice changes by  $\pm 10\%$  ( $DDF \pm 10\%$ ) and  $\pm 30\%$  ( $DDF \pm 30\%$ ), respectively, and temperature lapse rates and precipitation gradients changes by  $\pm 10\%$  ( $TP \pm 10\%$ ),  $\pm 30\%$  ( $TP \pm 30\%$ ) and  $\pm 50\%$  ( $TP \pm 50\%$ ), in which other parameters remain the same as before (Modelled).

unambiguous model calibration and the available data basis. In the Altai Mountains, only six glaciers have observed mass balance data, of which four glaciers are located in the same basin and three glaciers have short-term observations (Table 1). Therefore, the calibrated parameters by the model using the available data result in strong limits on the reliability and representativeness for the whole Altai Mountains. For the model parameters, values are assigned pseudo-randomly from our established methods. A somewhat surprising result from our simulation of surface mass balance is that the model performs well compared to the observations, although it slightly overestimates the magnitude of negative mass balances in some years due to the limited skill of the estimated DDFs for snow and ice. To quantify uncertainties resulted from the estimated parameters, we perform the following analyses for the surface mass balance modelling in the Aktru River Basin: one is to change the estimated DDFs for snow and ice by  $\pm 10\%$  and  $\pm 30\%$ , respectively, in which other parameters remain the same as before, the other is to change temperature lapse rates and precipitation gradients by  $\pm 10\%$ ,  $\pm 30\%$  and  $\pm 50\%$ , respectively, in which other parameters remain the same as before. As shown in Fig. 11, changing in the DDFs for snow and ice significantly increases the discrepancy between modelled and observed mass balances in some years, while changing in temperature lapse rate and

precipitation gradient slightly reduces the discrepancy, even changing in  $\pm 50\%$ . However, uncertainties in other years increase significantly with changing in these parameters (Fig. 11). These results indicate that the model parameters estimated through the methods mentioned above are acceptable for modelling surface mass balance in the Altai Mountains.

## 7. Conclusions

Glacier mass balance of the Altai Mountains is estimated for the 22-year period from 1990 to 2011 using a temperature-index glacier mass-balance model. The model is driven by daily data of air temperature and precipitation simulated by the WRF model. In addition to validate our model performance using observations on the five glaciers, we cross-validate the model performance during the period for which geodetic mass changes and area change data are available in different regions. Results indicate that mass loss rates have grown progressively for the entirety of the Altai glaciers since 1990, and about 81.3% of these glaciers experience considerable mass loss. The resulting mean annual specific mass balance is  $-0.69 \text{ m w.e}$  over the modelling period. In particular, a markedly rapid wastage of the Altai glaciers is found in recent years. Such glacier wastage provides a total meltwater discharge

of  $401.1 \times 10^8 \text{ m}^3$  for the entire study period and a contribution of  $0.0023 \text{ mm yr}^{-1}$  to sea-level rise.

We detect marked differences in surface mass balance for different regions and size classes. In addition to small areas distributed in the central and south-eastern parts of the Altai Mountains where mass gain occurs, glaciers in most parts of the region show considerable mass loss, especially in the western part. Small glaciers with the size class of  $0.1\text{--}0.5 \text{ km}^2$  experience the most considerable mass loss in the region over the past 22 years. The average mass balance sensitivities to a  $+1 \text{ }^\circ\text{C}$  rise in air temperature and a 10% increase in precipitation are about  $-0.56 \text{ m w.e. yr}^{-1} \text{ }^\circ\text{C}^{-1}$  and  $0.11 \text{ m w.e. yr}^{-1} (10\%)^{-1}$ , respectively, for the Altai glaciers. Temperature sensitivity of the glaciers is characterized by strong variability among different size classes, while precipitation sensitivity varies relatively little. Some regions, such as the Chuya Ridge and the Chinese Altai Mountains, experience considerable mass loss, although temperature and precipitation increase. In addition, temperature rise and precipitation decrease lead to dramatic mass loss of the glaciers located in the western part of the Altai Mountains.

### Acknowledgements

This work was supported by the National Natural Science Foundation of China (Grant No. 41671057), the National Basic Work Program of the Ministry of Science and Technology of China (Grant No. 2013FY111400), the Major Project of Chinese Academy of Sciences (Grant No. KZZD-EW-12-1), and MEXT (Japanese Ministry of Education, Culture, Sports, Science and Technology) through the Green Network of Excellence (GRENE) Arctic Climate Change Research Project. We thank Akiko Sakai of Nagoya University and the RGI consortium for providing glacier inventory data, and WGMS for glacier mass balance data for this work. We thank the editor, associate editor, and anonymous reviewers for their valuable comments.

### References

- Aizen, V.B., Aizen, E.M., Joswiak, D.R., Fujita, K., Takeuchi, N., Nikitin, S.A., 2006. Climatic and atmospheric circulation pattern variability from ice-core isotope/geochemistry records (Altai, Tien Shan and Tibet). *Ann. Glaciol.* 43 (1), 49–60.
- Arendt, A., Bliss, A., Bolch, T., Cogley, J.G., Gardner, A.S., Hagen, J.-O., Hock, R., Huss, M., Kaser, G., Kienholz, C., Pfeffer, W.T., Moholdt, G., Paul, F., Radić, V., Andreassen, L., Bajracharya, S., Barrand, N., Beedle, M., Berthier, E., Bhambri, R., Brown, I., Burgess, E., Burgess, D., Cawkwell, F., Chinn, T., Copland, L., Davies, B., De Angelis, H., Dolgova, E., Filbert, K., Forester, R., Fountain, A., Frey, H., Giffen, B., Glasser, N., Gurney, S., Hagg, W., Hall, D., Haritashya, U.K., Hartmann, G., Helm, C., Herreid, S., Howat, I., Kapustin, G., Khromova, T., König, M., Kohler, J., Kriegel, D., 2014. Randolph Glacier Inventory [v4.0]: a dataset of global glacier outlines. *Global Land Ice Measurements from Space*, Boulder, CO. Digital media: [http://www.glims.org/RGI/rgi40\\_dl.html](http://www.glims.org/RGI/rgi40_dl.html).
- Bahr, D.B., 1997. Width and length scaling of glaciers. *J. Glaciol.* 43 (145), 557–562.
- Bahr, D.B., Meier, M.F., Peckham, S.D., 1997. The physical basis of glacier volume-area scaling. *J. Geophys. Res.* 102 (B9), 20355–20362.
- Bezuglova, N.N., Zinchenko, G.S., Malygina, N.S., Papina, T.S., Barlyaeva, T.V., 2012. Response of high-mountain Altai thermal regime to climate global warming of recent decades. *Theor. Appl. Climatol.* 110 (4), 595–605.
- Braithwaite, R.J., Zhang, Y., 2000. Sensitivity of mass balance of five Swiss glaciers to temperature changes assessed by tuning a degree-day model. *J. Glaciol.* 46 (152), 7–14.
- Braithwaite, R.J., Zhang, Y., Raper, S.C.B., 2002. Temperature sensitivity of the mass balance of mountain glaciers and ice caps as a climatological characteristic. *Z. Glaciol. Glazialgeol.* 38, 35–61.
- Chen, J., Ohmura, A., 1990. Estimation of Alpine glacier water resources and their change since the 1870s. *IAHS Publ.* 193, 127–135.
- Collier, E., Mölg, T., Maussion, F., Scherer, D., Mayer, C., Bush, A.B.G., 2013. High-resolution interactive modelling of the mountain glacier-atmosphere interface: an application over the Karakoram. *Cryosphere* 7, 779–795.
- Cuffey, K.M., Paterson, W.S.B., 2010. *The Physics of Glaciers*. Butterworth-Heinemann, Oxford.
- Dyurgerov, M.B., 2010. *Reanalysis of Glacier Changes: From the IGY to the IPY, 1960–2008*. Institute of Arctic and Alpine Research, University of Colorado at Boulder, Boulder, Colorado, USA.
- Fang, J.Y., Yoda, K., 1988. Climate and vegetation in China (I), Changes in the altitudinal lapse rate of temperature and distribution of sea level temperature. *Ecol. Res.* 3 (1), 37–51.
- Fujita, K., Ageta, Y., 2000. Effect of summer accumulation on glacier mass balance on the Tibetan Plateau revealed by mass-balance model. *J. Glaciol.* 46 (153), 244–252.
- Gao, Y., Xu, J., Chen, D., 2015. Evaluation of WRF mesoscale climate simulations over the Tibetan plateau during 1979–2011. *J. Climate* 28 (7), 2823–2841.
- Hartmann, D.L., Klein Tank, A.M.G., Rusticucci, M., Alexander, L.V., Brönnimann, S., Charabi, Y., Dentener, F.J., Dlugokencky, E.J., Easterling, D.R., Kaplan, A., Soden, B. J., Thorne, P.W., Wild, M., Zhai, P.M., 2013. *Observations: atmosphere and surface*. In: Stocker, T.F., Qin, D., Plattner, G.-K., Tignor, M., Allen, S.K., Boschung, J., Nauels, A., Xia, Y., Bex, V., Midgley, P.M. (Eds.), *Climate Change 2013: The Physical Science Basis. Contribution of Working Group I to the Fifth Assessment Report of the Intergovernmental Panel on Climate Change*. Cambridge University Press, Cambridge, United Kingdom and New York, NY, USA.
- Henderson, K., Laube, A., Gaggeler, H.W., Olivier, S., Papina, T., Schwikowski, M., 2006. Temporal variations of accumulation and temperature during the past two centuries from Belukha ice core. *Siberian Altai. J. Geophys. Res.* 111, D03104.
- Hirabayashi, Y., Döll, P., Kanae, S., 2010. Global-scale modeling of glacier mass balances for water resources assessments: Glacier mass changes between 1948 and 2006. *J. Hydrol.* 390, 245–256.
- Hirabayashi, Y., Zhang, Y., Watanabe, S., Koirala, S., Kanae, S., 2013. Projection of glacier mass changes under a high-emission climate scenario using the global glacier model HYOGA2. *Hydrol. Res. Lett.* 7 (1), 6–11.
- Hock, R., 2003. Temperature index melt modelling in mountain areas. *J. Hydrol.* 282, 104–115.
- Immerzeel, W.W., Petersen, L., Ragetti, S., Pellicciotti, F., 2014. The importance of observed gradients of air temperature and precipitation for modeling runoff from a glacierized watershed in the Nepalese Himalayas. *Water Res. Res.* 50, 2212–2226.
- Kadota, T., Gombo, D., 2007. Recent glacier variations in Mongolia. *Ann. Glaciol.* 46, 185–188.
- Kadota, T., Gombo, D., Kalsan, P., Namgur, D., 2011. Glaciological research in the Mongolian Altai, 2003–2009. *Bull. Glaciol. Res.* 29, 41–50.
- Kalugin, I., Daryin, A., Smolyaninova, L., Andreev, A., Diekmann, B., Khlystov, O., 2007. 800-yr-long records of annual air temperature and precipitation over southern Siberia inferred from Teletskoye Lake sediments. *Quat. Res.* 67 (3), 400–410.
- Kaser, G., Großhauser, M., Marzeion, B., 2010. Contribution potential of glaciers to water availability in different climate regimes. *PNAS* 107 (47), 20223–20227.
- Kitabata, H., Sugiura, K., Kadota, T., 2014. Analysis of Climate Trends in the Altai Mountains Between 1988 and 2012. Abstract #C41B-0346 presented at 2014 Fall Meeting, AGU, San Francisco, Calif., 15–20 Dec.
- Klinge, M., Böhrer, J., Lehmkühl, F., 2003. Climate pattern, snow and timberlines in the Altai mountains, central Asia. *Erdkunde* 57 (4), 296–307.
- Konya, K., Kadota, T., Nakazawa, F., Davaa, G., Purevdagva, K., Yabuki, H., Ohata, T., 2013. Surface mass balance of the Potanin Glacier in the Mongolian Altai Mountains and comparison with Russian Altai glaciers in 2005, 2008, and 2009. *Bull. Glaciol. Res.* 31, 9–18.
- Krumwiede, B.S., Kamp, U., Leonard, G.J., Kargel, J.S., Dashtseren, A., Walther, M., 2014. Recent glacier changes in the Mongolia Altai Mountains: Case studies from Munkh Khairkhan and Tavan Bogd. In: Kargel, J.S., Leonard, G.J., Bishop, M.P., Käb, A., Raup, B. (Eds.), *Global Land Ice Measurements from Space*. Springer-Verlag, Berlin Heidelberg.
- Lang, C., Fettweis, X., Ericum, M., 2015. Stable climate and surface mass balance in Svalbard over 1979–2013 despite the Arctic warming. *Cryosphere* 9 (1), 83–101.
- Li, X., Wang, L., Chen, D., Yang, K., Xue, B., Sun, L., 2013. Near-surface air temperature lapse rates in the mainland China during 1962–2011. *J. Geophys. Res.* 118 (14), 7505–7515.
- Li, Z., Li, K., Wang, L., 2010. Study on recent glacier changes and their impact on water resources in Xinjiang. *North Western China. Quat. Sci.* 30 (1), 96–106.
- Ligtenberg, S.R.M., Berg, W.J., Broeke, M.R., Rae, J.G.L., Meijgaard, E., 2013. Future surface mass balance of the Antarctic ice sheet and its influence on sea level change, simulated by a regional atmospheric climate model. *Clim. Dyn.* 41 (3–4), 867–884.
- Liu, Q., Liu, S., 2015. Response of glacier mass balance to climate change in the Tianshan Mountains during the second half of the twentieth century. *Clim. Dyn.* 46 (1), 301–316.
- Lutz, W., Butz, W.P., Samir, K.C., 2014. *World Population and Human Capital in the Twenty-First Century*. Oxford University Press, Oxford.
- Machguth, H., Paul, F., Kotlarski, S., Hoelzle, M., 2009. Calculating distributed glacier mass balance for the Swiss Alps from regional climate model output: A methodical description and interpretation of the results. *J. Geophys. Res.* 114, D19106.
- Malygina, N., Papina, T., Kononova, N., Barlyaeva, T., 2017. Influence of atmospheric circulation on precipitin in Altai Mountains. *J. Mt. Sci.* 14 (1), 46–59.
- Marzeion, B., Jarosch, A.H., Hofer, M., 2012. Past and future sea-level change from the surface mass balance of glaciers. *Cryosphere* 6, 1295–1322.
- Maussion, F., Scherer, D., Finkelnburg, R., Richters, J., Yang, W., Yao, T., 2011. WRF simulation of a precipitation event over the Tibetan Plateau, China—an assessment using remote sensing and ground observations. *Hydrol. Earth Syst. Sci.* 15 (6), 1795–1817.

- Mölg, T., Kaser, G., 2011. A new approach to resolving climate-cryosphere relations: downscaling climate dynamics to glacier-scale mass and energy balance without statistical scale linking. *J. Geophys. Res.* 116, D16101.
- Mölg, T., Maussion, F., Scherer, D., 2013. Mid-latitude westerlies as a driver of glacier variability in monsoonal High Asia. *Nat. Clim. Change* 4 (1), 68–73.
- Mölg, T., Maussion, F., Yang, W., Scherer, D., 2012. The footprint of Asian monsoon dynamics in the mass and energy balance of a Tibetan glacier. *Cryosphere* 6, 1445–1461.
- Möller, M., Obleitner, F., Reijmer, C.H., Pohjola, V.A., Glowacki, P., Kohler, J., 2016. Adjustment of regional climate model output for modeling the climatic mass balance of all glaciers on Svalbard. *J. Geophys. Res.* 121 (10), 5411–5429.
- Narozhniy, Y., Zemtsov, V., 2011. Current state of the Altai Glaciers (Russia) and trends over the period of instrumental observations 1952–2008. *AMBIO* 40 (6), 575–588.
- Nuimura, T., Sakai, A., Taniguchi, K., Nagai, H., Lamsal, D., Tsutaki, S., Kozawa, A., Hoshina, Y., Takenaka, S., Omiya, S., Tsunematsu, K., Tshering, P., Fujita, K., 2015. The GAMDAM glacier inventory: a quality-controlled inventory of Asian glaciers. *Cryosphere* 9 (3), 849–864.
- Oerlemans, J., Fortuin, J.P.F., 1992. Sensitivity of glaciers and small ice caps to greenhouse warming. *Science* 258, 115–117.
- Okamoto, S., Fujita, K., Narita, H., Uetake, J., Takeuchi, N., Miyake, T., Nakazawa, F., Aizen, V.B., Nikitin, S.A., Nakawo, M., 2011. Reevaluation of the reconstruction of summer temperatures from melt features in Belukha ice cores, Siberian Altai. *J. Geophys. Res.* 116, D02110.
- Pan, C.G., 2013. Inventory of Mongolian Glaciers for the Global Land Ice Measurements from Space (GLIMS) Program (PhD thesis). The University of Montana.
- Panagiotopoulos, F., Shahgedanova, M., Hannachi, A., Stephenson, D.B., 2005. Observed trends and teleconnections of the siberian high: a recently declining center of action. *J. Climate* 18 (9), 1411–1422.
- Petersen, L., Pellicciotti, F., 2011. Spatial and temporal variability of air temperature on a melting glacier: atmospheric controls, extrapolation methods and their effect on melt modeling, Juncal Norte Glacier, Chile. *J. Geophys. Res.* 116, D23109.
- Priess, J.A., Schweitzer, C., Wimmer, F., Batkhisig, O., Mimler, M., 2011. The consequences of land-use change and water demands in Central Mongolia. *Land Use Policy* 28 (1), 4–10.
- Pritchard, H.D., 2017. Asia's glaciers are a regionally important buffer against drought. *Nature* 545 (7653), 169–174.
- Radić, V., Hock, R., 2010. Regional and global volumes of glaciers derived from statistical upscaling of glacier inventory data. *J. Geophys. Res.* 115, F01010.
- Radić, V., Hock, R., 2011. Regionally differentiated contribution of mountain glaciers and ice caps to future sea-level rise. *Nat. Geosci.* 4, 91–94.
- Radić, V., Hock, R., Oerlemans, J., 2008. Analysis of scaling methods in deriving future volume evolutions of valley glaciers. *J. Glaciol.* 54 (187), 601–612.
- Shahgedanova, M., Nosenko, G., Khromova, T., Muraveyev, A., 2010. Glacier shrinkage and climatic change in the Russian Altai from the mid-20th century: An assessment using remote sensing and PRECIS regional climate model. *J. Geophys. Res.* 115, D16107.
- Skamarock, W., Klemp, J.B., Dudhia, J., Gill, D.O., Barker, D., Duda, M.G., Huang, X.-Y., Wang, W., 2008. A Description of the Advanced Research WRF Version 3. NCAR Technical Note NCAR/TN-475+STR, doi: 10.5065/D68S4MVH.
- Skamarock, W.C., Klemp, J.B., 2008. A time-split nonhydrostatic atmospheric model for weather research and forecasting applications. *J. Comput. Phys.* 227, 3465–3485.
- Sugiura, K., Kitabata, H., Kadota, T., 2014. Validation of snow cover simulated by the Weather Research and Forecasting (WRF) model using in-situ snow survey data in the Altai Mountains. Abstract #C43A-0369 presented at 2014 Fall Meeting, AGU, San Francisco, Calif., 15–20 Dec.
- Surazakov, A.B., Aizen, V.B., Aizen, E.M., Nikitin, S.A., 2007. Glacier changes in the Siberian Altai Mountains, Ob river basin, (1952–2006) estimated with high resolution imagery. *Environ. Res. Lett.* 2 (4), 045017.
- Syromyatina, M.V., Kurochkin, Y.N., Bliakharskii, D.P., Chistyakov, K.V., 2015. Current dynamics of glaciers in the Tavan Bogd Mountains (Northwest Mongolia). *Environ. Earth Sci.* 74 (3), 1905–1914.
- Tachikawa, T., Kaku, M., Iwasaki, A., Gesch, D., Oimoen, M., Zhang, Z., Danielson, J., Krieger, T., Curtis, B., Haase, J., Abrams, M., Crippen, R., Carabajal, C., 2011. ASTER Global Digital Elevation Model Version 2—Summary of Validation Results. Technical report, NASA Land Processes Distributed Active Archive Center and the Joint Japan-US ASTER Science Team.
- Viviroli, D., Archer, D., Buytaert, W., Fowler, H., Greenwood, G., Hamlet, A., Huang, Y., Koboltschnig, G., Litaor, M., Lopez-Moreno, J., 2011. Climate change and mountain water resources: overview and recommendations for research, management and policy. *Hydrol. Earth Syst. Sci.* 15 (2), 471–504.
- Wang, X.L., Cho, H.-R., 1997. Spatial-temporal structures of trend and oscillatory variabilities of precipitation over northern Eurasia. *J. Climate* 10 (9), 2285–2298.
- Wei, J., Liu, S., Xu, J., Guo, W., Bao, W., Shangguan, D., Jiang, Z., 2015. Mass loss from glaciers in the Chinese Altai Mountains between 1959 and 2008 revealed based on historical maps, SRTM, and ASTER images. *J. Mt. Sci.* 12 (2), 330–343.
- WGMS, 2014. Fluctuations of Glaciers Database World Glacier Monitoring Service, Zurich, Switzerland, doi:10.5904/wgms-fog-2014-09.
- Woodward, J., Sharp, M., Arendt, A., 1997. The influence of superimposed-ice formation on the sensitivity of glacier mass balance to climate change. *Ann. Glaciol.* 24, 186–190.
- Wright, A.P., Wadham, J.L., Siegert, M.J., Luckman, A., Kohler, J., Nuttall, A.M., 2007. Modeling the refreezing of meltwater as superimposed ice on a high Arctic glacier: A comparison of approaches. *J. Geophys. Res.* 112, F04016.
- Yao, X., Liu, S., Guo, W., Huai, B., Sun, M., Xu, J., 2012. Glacier change of Altay mountain in China from 1960 to 2009—based on the second glacier inventory of China. *J. Nat. Resour.* 27 (10), 1734–1745 (In Chinese with English abstract).
- Zhang, Y., Enomoto, H., Ohata, T., Kitabata, H., Kadota, T., Hirabayashi, Y., 2016. Projections of glacier change in the Altai Mountains under twenty-first century climate scenarios. *Clim. Dyn.* 47, 2935–2953.
- Zhang, Y., Liu, S., Ding, Y., 2006. Observed degree-day factors and their spatial variation on glaciers in western China. *Ann. Glaciol.* 46, 301–306.
- Zhang, Y., Sun, M., Liu, Q., Liu, S., 2017a. Glacier mass balance and runoff modelling. In: Liu, S., Zhang, Y., Liu, Q., Sun, M. (Eds.), Study on the impact of climate change on glacier and its risk. Science Press, Beijing, pp. 108–112 (In Chinese).
- Zhang, Y., Enomoto, H., Ohata, T., Kadota, T., Shirakawa, T., Takeuchi, N., 2017b. Surface mass balance on Glacier No. 31 in the Suntar-Khayata Range, eastern Siberia, from 1951 to 2014. *J. Mt. Sci.* 14 (3), 501–512.